

GRAVITATIONAL LENSING

24 - USING STRONG LENSES (2)

Massimo Meneghetti
AA 2018-2019

2) MEASURE COSMOLOGICAL PARAMETERS

COSMOGRAPHY WITH TIME DELAYS

Treu & Marshall, 2016

$$\text{Time delay distance} \propto \frac{1}{H_0}$$

$$\tau(\theta) = \frac{D_{\Delta t}}{c} \cdot \Phi(\theta, \beta),$$

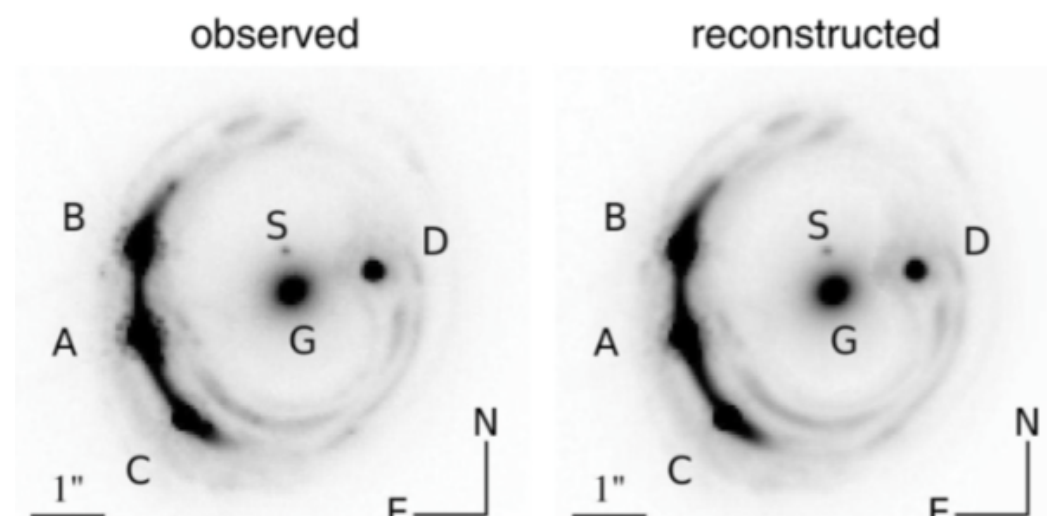
$$\text{where } \Phi(\theta) = \frac{1}{2} (\theta - \beta)^2 - \psi(\theta).$$

*Distances encode
information on additional
cosmological parameters!*

$$D_{\Delta t}(z_d, z_s) = (1 + z_d) \frac{D_d D_s}{D_{ds}}$$

*From the lens mass
distribution*

- Needed ingredients:
 - Time delays
 - lens mass distribution



RXJ1131

THE HUBBLE CONSTANT FROM TIME DELAYS

ON THE POSSIBILITY OF DETERMINING HUBBLE'S PARAMETER
AND THE MASSES OF GALAXIES FROM THE GRAVITATIONAL
LENS EFFECT*

Sjur Refsdal

(Communicated by H. Bondi)

(Received 1964 January 27)

Summary

The gravitational lens effect is applied to a supernova lying far behind and close to the line of sight through a distant galaxy. The light from the supernova may follow two different paths to the observer, and the difference Δt in the time of light travel for these two paths can amount to a couple of months or more, and may be measurable. It is shown that Hubble's parameter and the mass of the galaxy can be expressed by Δt , the red-shifts of the supernova and the galaxy, the luminosities of the supernova "images" and the angle between them. The possibility of observing the phenomenon is discussed.

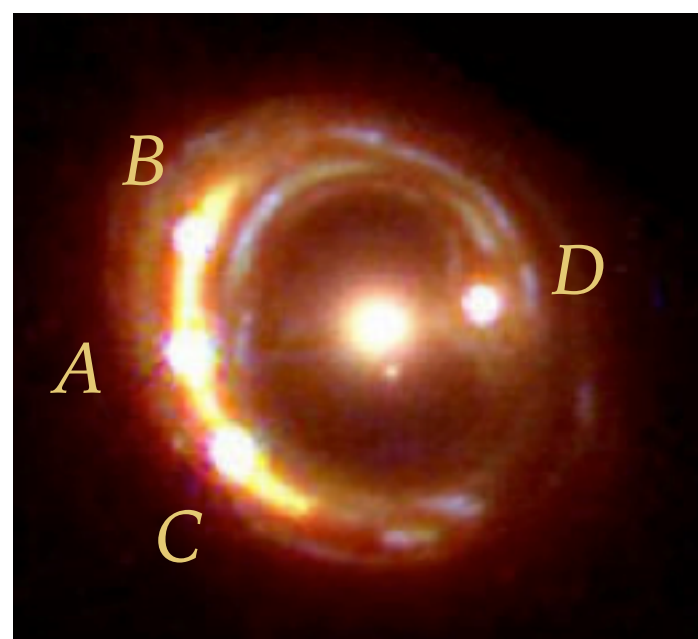
TABLE 2
HUBBLE CONSTANT FROM EACH LENS SYSTEM

Lens Name	h (1 σ Range)	$h = H_0/100$
B0218+357.....	0.21 (...)	
HE 0435–1223.....	1.02 (0.70–1.39)	
RX J0911+0551.....	0.96 (0.75–1.21)	
SBS 0909+532.....	0.84 (0.47–)	
FBQ 0951+2635	0.67 (0.56–0.81)	
Q0957+561	0.99 (0.82–1.17)	
HE 1104–1805.....	1.04 (0.92–1.22)	
PG 1115+080.....	0.66 (0.49–0.84)	
RX J1131–1231	0.79 (0.59–1.03)	
B1422+231.....	0.16 (–0.36)	
SBS 1520+530.....	0.53 (0.46–0.61)	
B1600+434.....	0.65 (0.54–0.77)	
B1608+656.....	0.89 (0.77–1.20)	
SDSS J1650+4251	0.53 (0.44–0.63)	
PKS 1830–211.....	0.88 (0.58–)	
HE 2149–2745.....	0.69 (0.57–0.82)	
All	0.70 (0.68–0.73)	

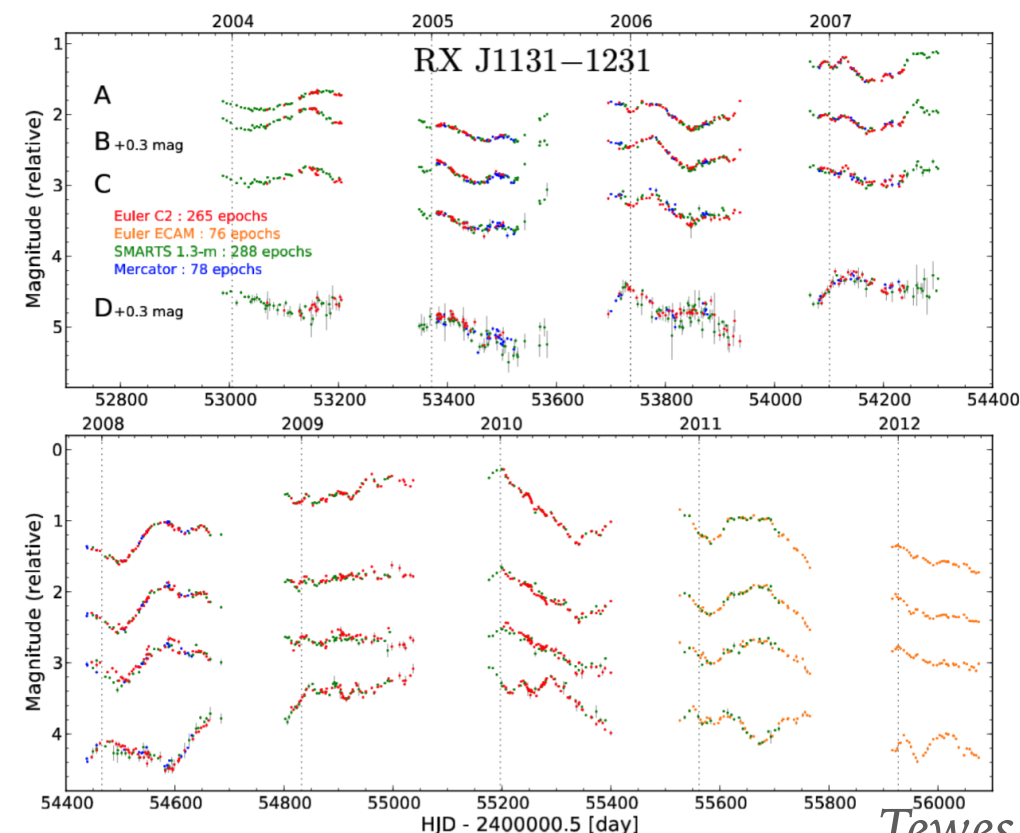
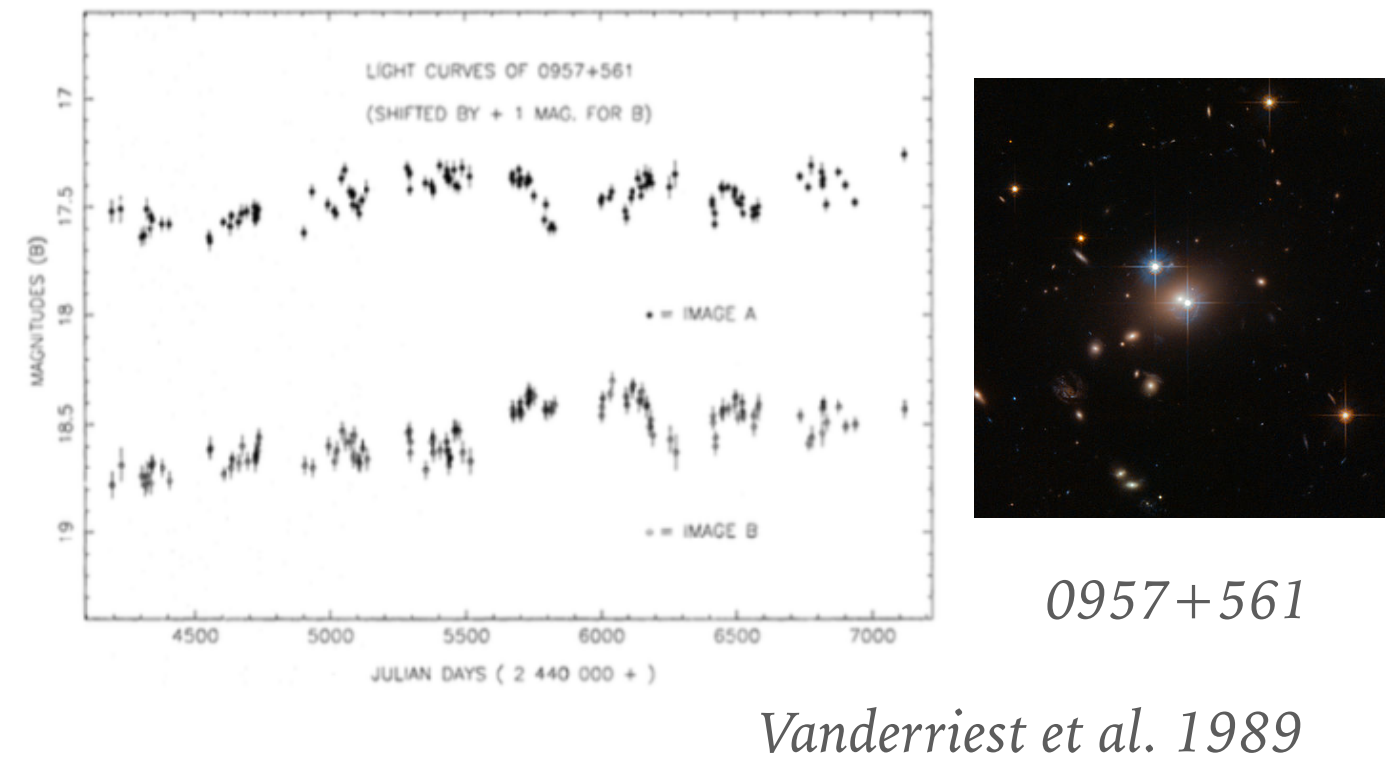
NOTE.—The Hubble constant and its error are estimated from the effective χ^2 .

CURRENT MEASUREMENTS OF TIME DELAYS

Enormous progress in the quality of the light curves since the first measurements thanks to dedicated networks of telescopes. For example: the COSMOGRAIL project measured time delays with precision $<4\%$ for 5 lenses

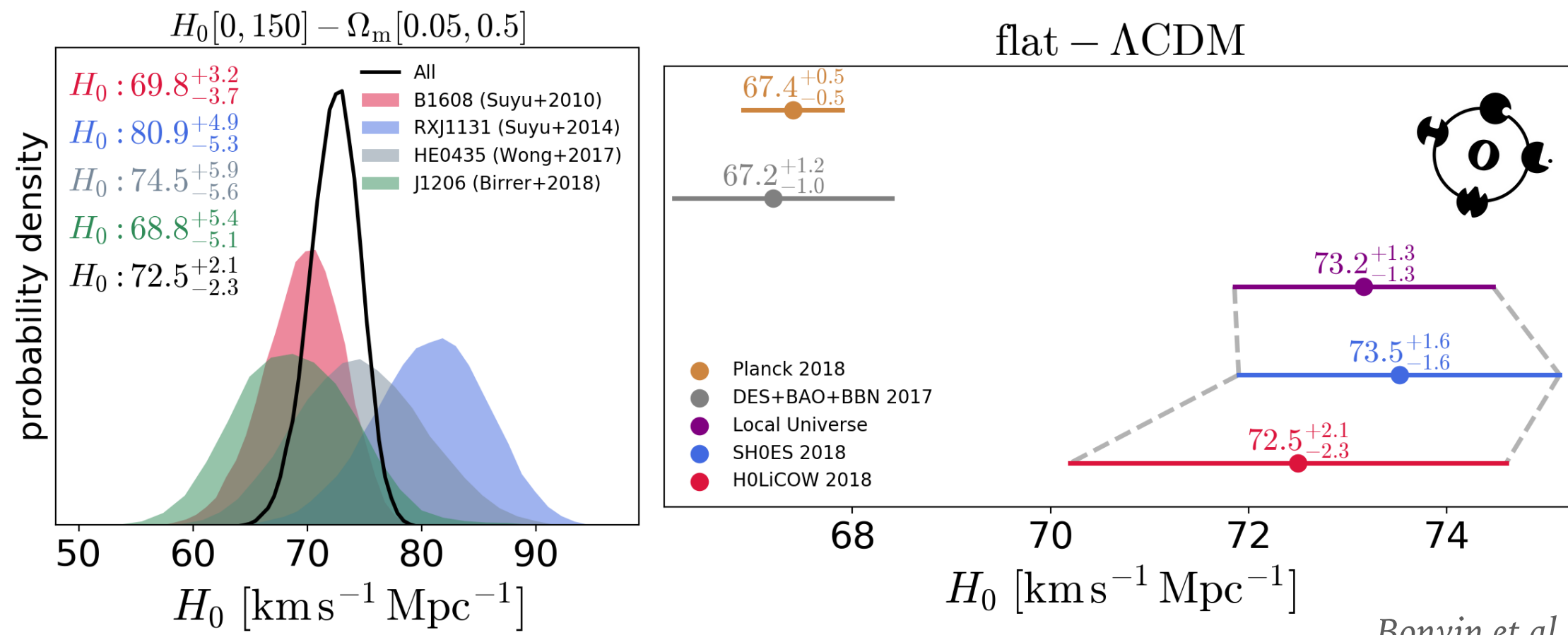


RXJ1131



THE HOLICOW COLLABORATION (H₀ LENSES IN COSMOGRAIL'S WELLSPRING)

- focussing on the lenses with the best constrained time delays
- recently published results based on four multiply imaged QSOs
- they measure $H_0 = 72.5^{+2.1}_{-2.3} \text{ km/s/Mpc}$ in a LCDM cosmology
- results are in agreement with cepheids and SNe (SH0ES), but in tension with the recent CMB predictions or with BAO+WL



COSMOGRAPHY WITH SOURCES AT MULTIPLE REDSHIFTS

- Even if time delay measurements are not available, the sensitivity to cosmology remains in the astrometric constraints
- With only one lensed source, the distance ratio is degenerate with the mass distribution
- With constraints from multiple sources, one can try to break the degeneracy by measuring the so called “family ratio”
- This technique could be used in the case of e.g. **compound lenses**, but also in **galaxy clusters**, where it is easier to observe lensing of many sources

$$\vec{\beta} = \vec{\theta} - \frac{D_{LS}}{D_S} \hat{\vec{\alpha}}(\vec{\theta})$$

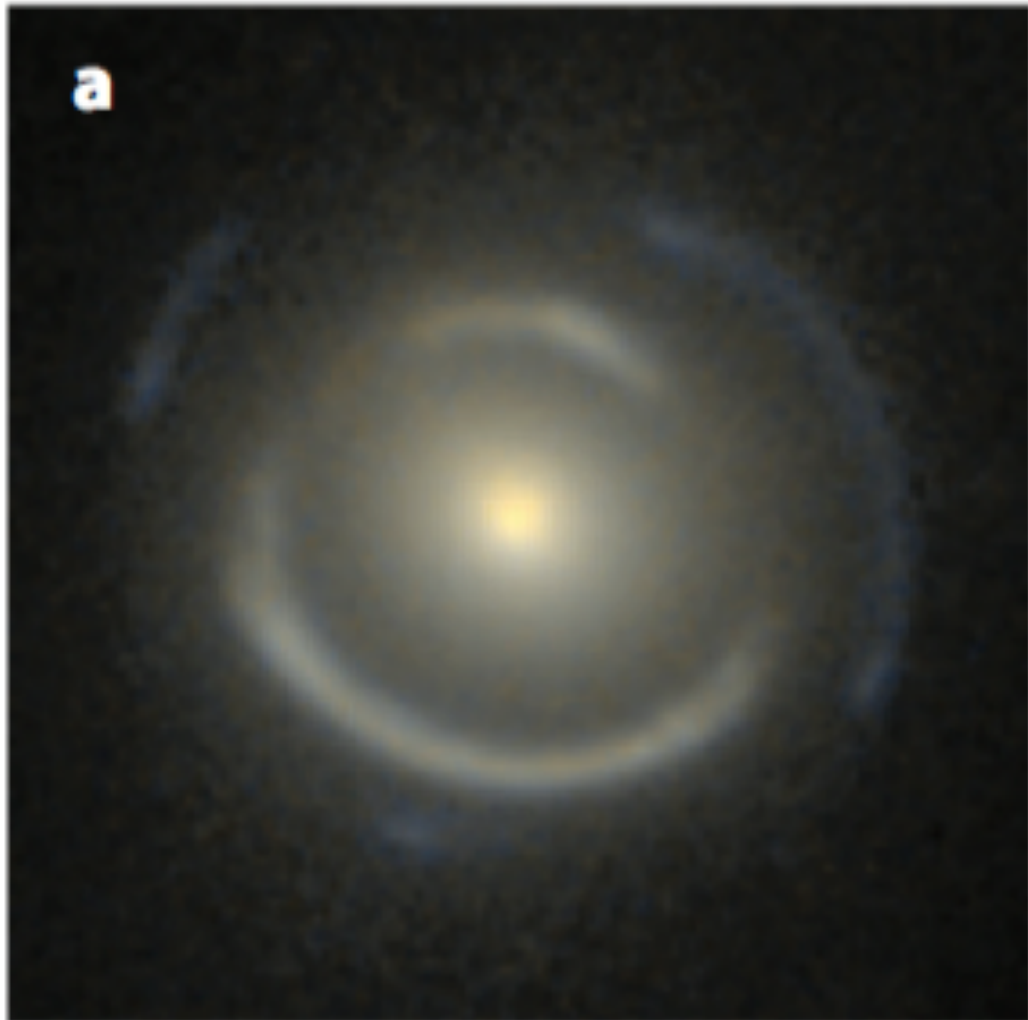
depends on cosmology

depends on the mass distr.

$$\Xi_{S1,S2}(\vec{\pi}) = \frac{D_{LS,1}(\vec{\pi})D_{S,2}(\vec{\pi})}{D_{LS,2}(\vec{\pi})D_{S,1}(\vec{\pi})}$$

EXAMPLE:

SDSSJ0946 + 1006



Suppose the lens is well described by a SIS model:

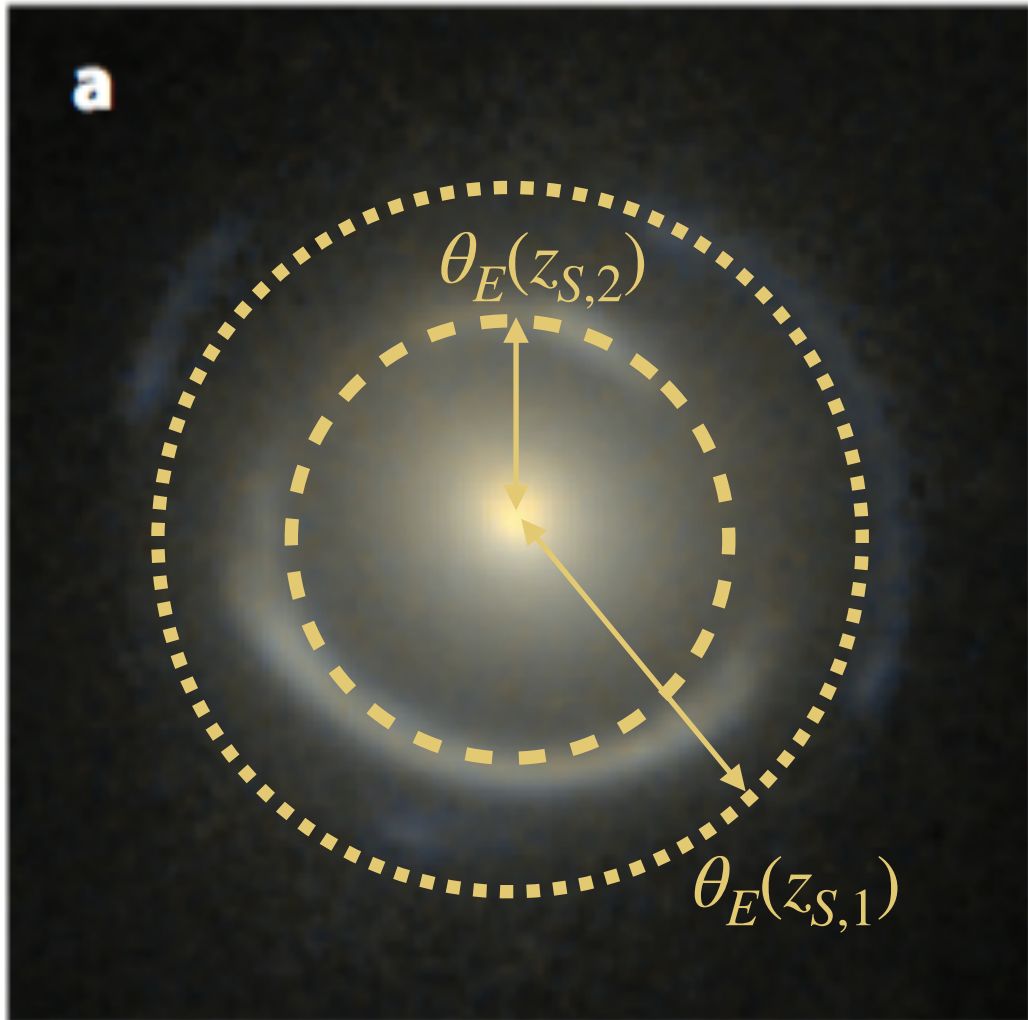
$$\theta_E(z_S) = 4\pi \left(\frac{\sigma_v}{c}\right)^2 \frac{D_{LS}(z_L, z_S)}{D_S(z_S)}$$

With two Einstein rings:

$$\frac{\theta_E(z_{S,1})}{\theta_E(z_{S,2})} = \frac{D_{LS,1}}{D_{S,1}} \frac{D_{S,2}}{D_{LS,2}} \equiv \Xi(z_{S,1}, z_{S,2})$$

EXAMPLE:

SDSSJ0946 + 1006



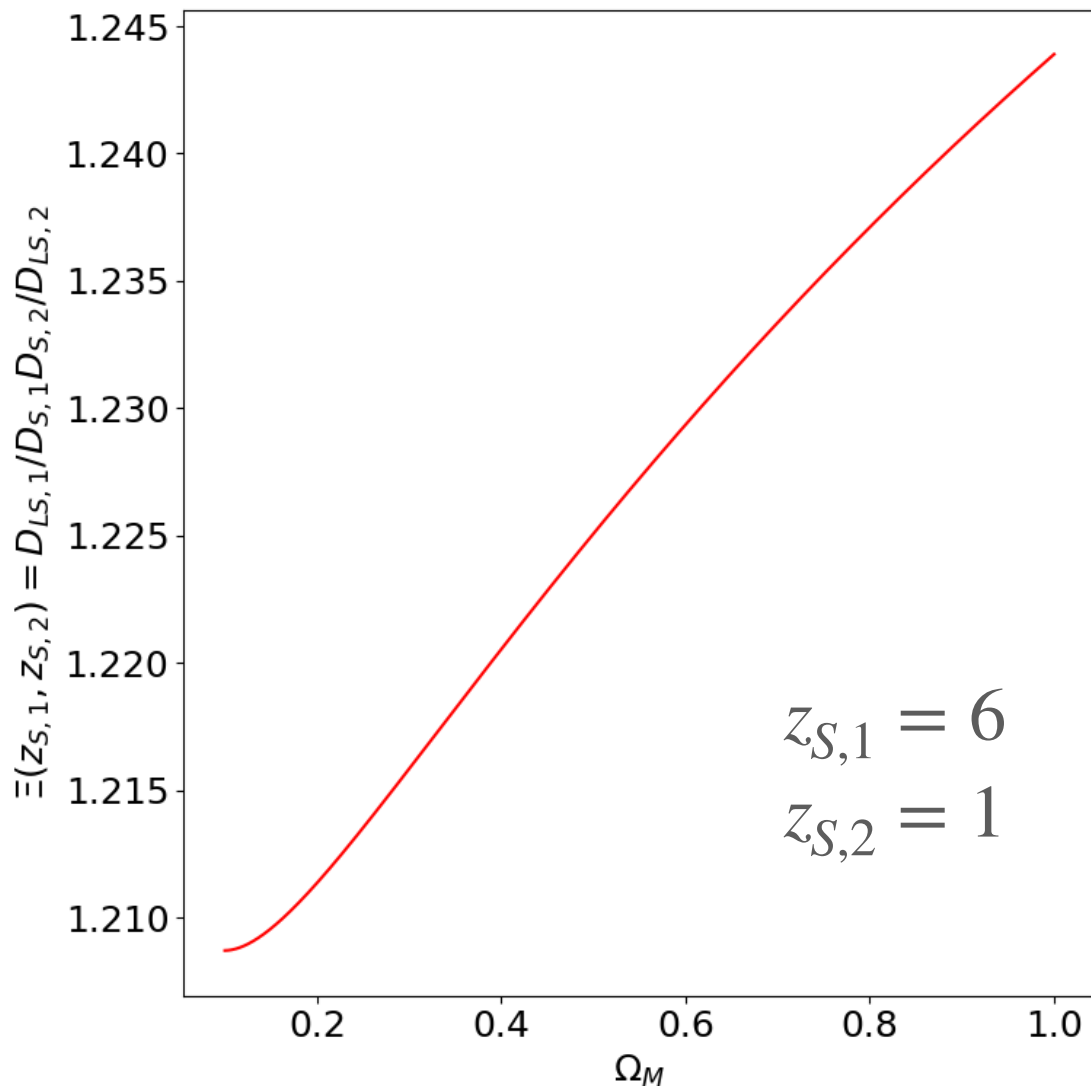
Suppose the lens is well described by a SIS model:

$$\theta_E(z_S) = 4\pi \left(\frac{\sigma_v}{c}\right)^2 \frac{D_{LS}(z_L, z_S)}{D_S(z_S)}$$

With two Einstein rings:

$$\frac{\theta_E(z_{S,1})}{\theta_E(z_{S,2})} = \frac{D_{LS,1}}{D_{S,1}} \frac{D_{S,2}}{D_{LS,2}} \equiv \Xi(z_{S,1}, z_{S,2})$$

EXAMPLE:



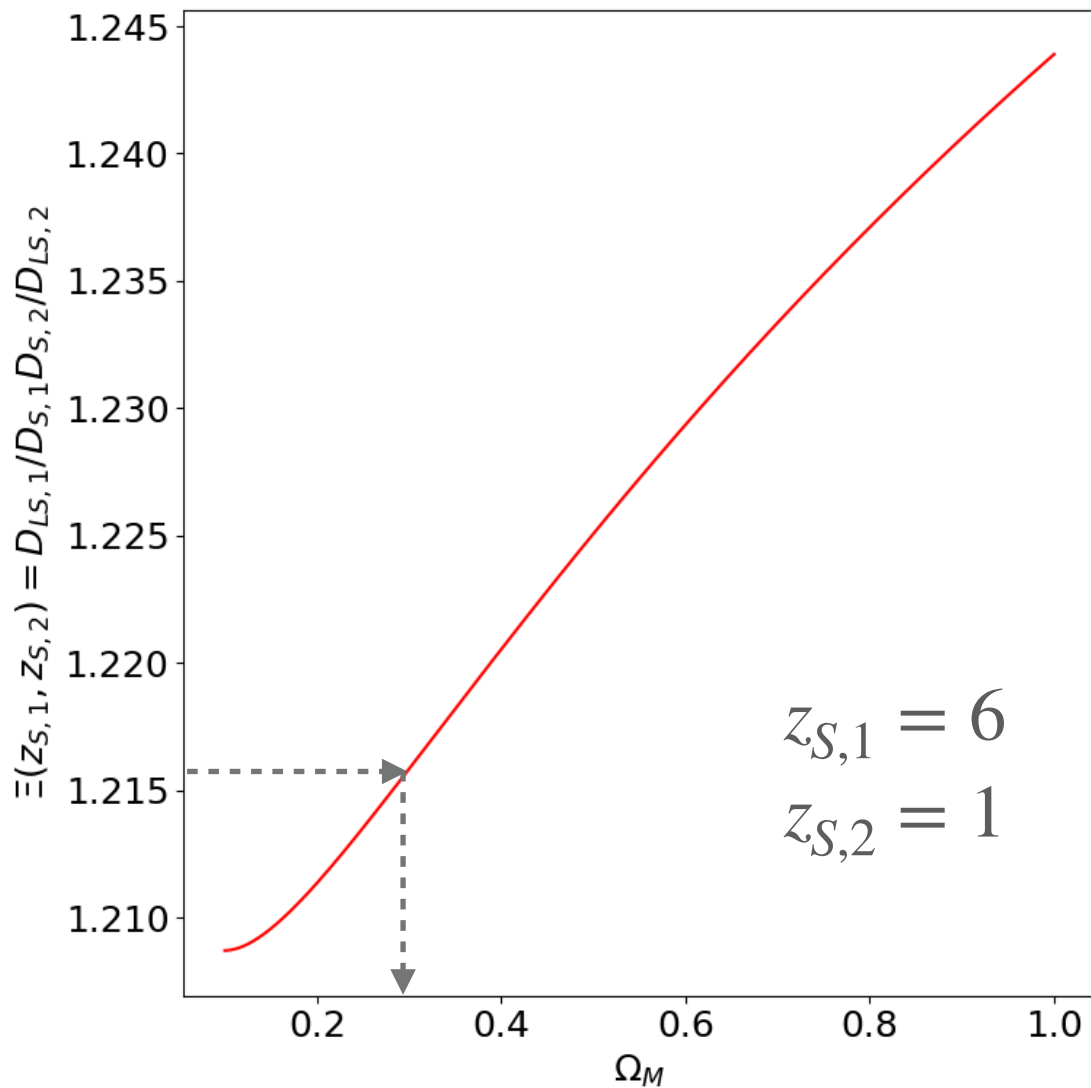
Suppose the lens is well described by a SIS model:

$$\theta_E(z_S) = 4\pi \left(\frac{\sigma_v}{c}\right)^2 \frac{D_{LS}(z_L, z_S)}{D_S(z_S)}$$

With two Einstein rings:

$$\frac{\theta_E(z_{S,1})}{\theta_E(z_{S,2})} = \frac{D_{LS,1}}{D_{S,1}} \frac{D_{S,2}}{D_{LS,2}} \equiv \Xi(z_{S,1}, z_{S,2})$$

EXAMPLE:



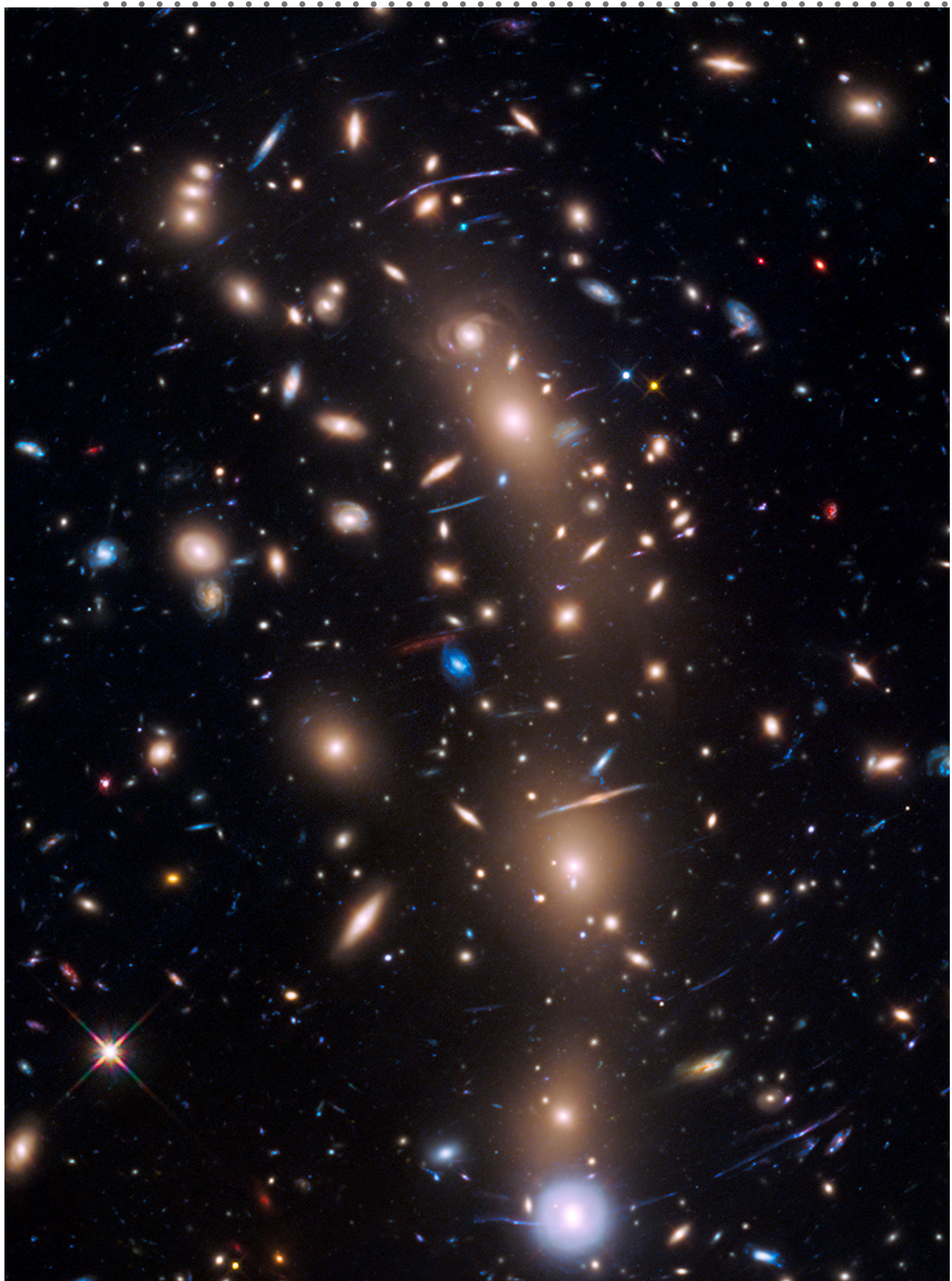
Suppose the lens is well described by a SIS model:

$$\theta_E(z_S) = 4\pi \left(\frac{\sigma_v}{c}\right)^2 \frac{D_{LS}(z_L, z_S)}{D_S(z_S)}$$

With two Einstein rings:

$$\frac{\theta_E(z_{S,1})}{\theta_E(z_{S,2})} = \frac{D_{LS,1}}{D_{S,1}} \frac{D_{S,2}}{D_{LS,2}} \equiv \Xi(z_{S,1}, z_{S,2})$$

3) EXPLORING THE VERY DISTANT AND FAINT UNIVERSE



- Several galaxy clusters have been observed with HST or with ground based facilities looking for lensed galaxies
- Several SL focused Hubble MCT programs since 2012
- CLASH (PI Postman, 25 clusters, 525 orbits, 16 bands)
- **Frontier-Fields (PI Lotz, 6 clusters, 840 orbits, 7 bands)**
- deep, high-resolution imaging from UV to NIR
- $m_{\text{int}} = m_{\text{obs}} + 2.5 \log 10(\mu)$

ACS: (70 orbits per position)			WFC3/IR: (70 orbits per position)		
Filter	Orbits	AB_mag	Filter	Orbits	AB_mag
F435W	18	28.8	F105W	24	28.9
F606W	10	28.8	F125W	12	28.6
F814W	42	29.1	F140W	10	28.6
			F160W	24	28.7

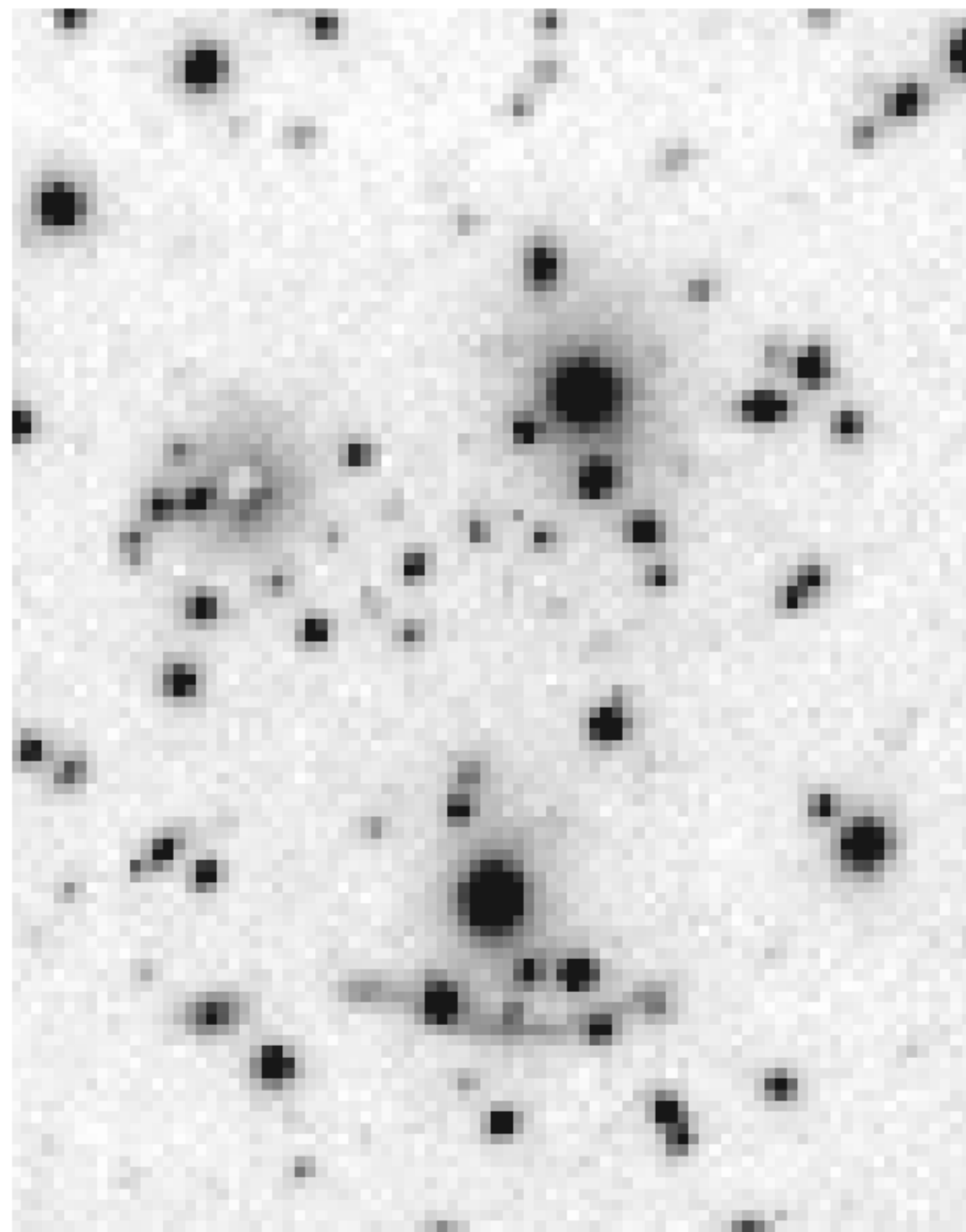
3) EXPLORING THE VERY DISTANT AND FAINT UNIVERSE



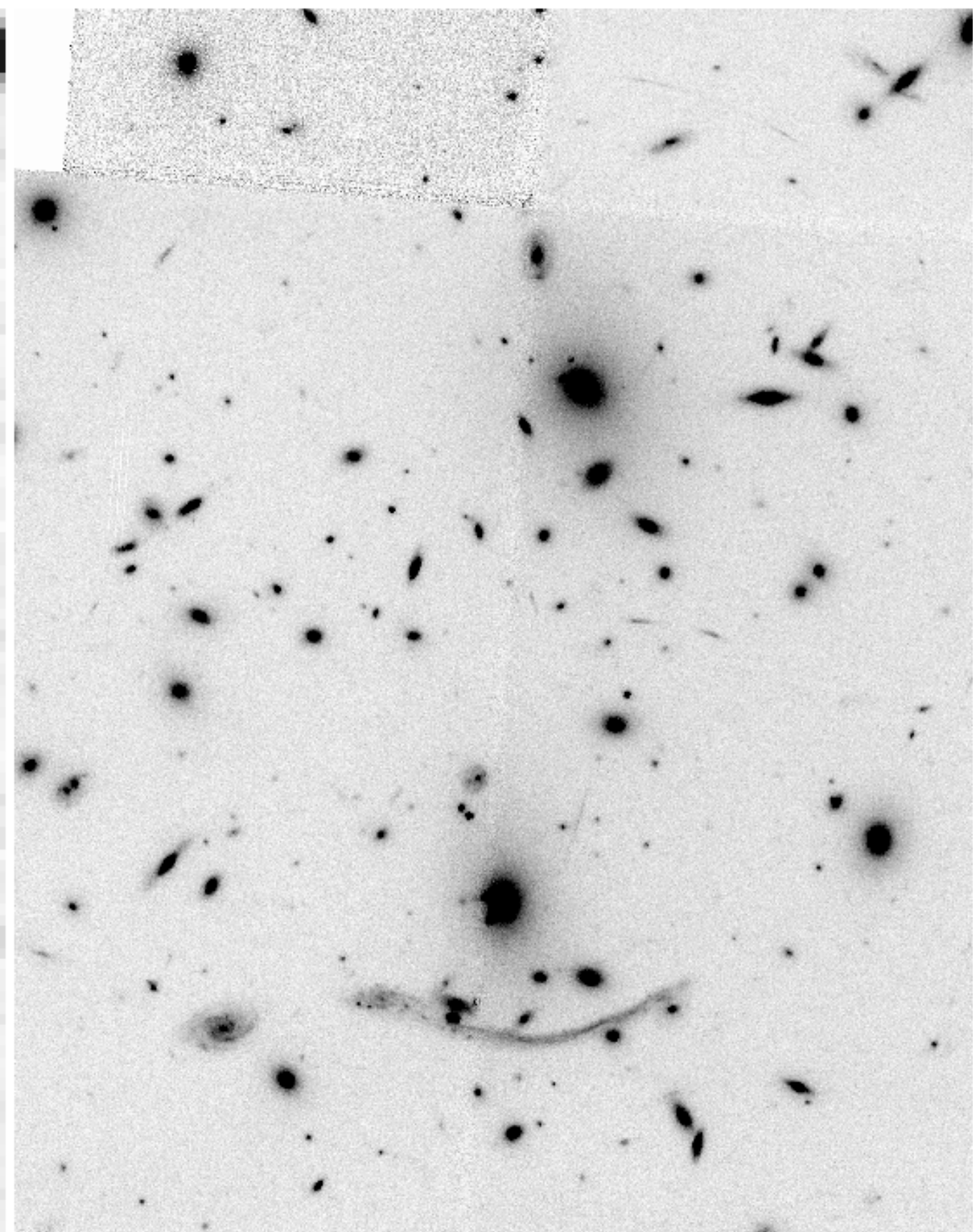
- Several galaxy clusters have been observed with HST or with ground based facilities looking for lensed galaxies
- Several SL focused Hubble MCT programs since 2012
- CLASH (PI Postman, 25 clusters, 525 orbits, 16 bands)
- **Frontier-Fields (PI Lotz, 6 clusters, 840 orbits, 7 bands)**
- deep, high-resolution imaging from UV to NIR
- $m_{int} = m_{obs} + 2.5 \log 10(\mu)$

ACS: (70 orbits per position)			WFC3/IR: (70 orbits per position)		
Filter	Orbits	AB mag	Filter	Orbits	AB mag
F435W	18	28.8	F105W	24	28.9
F606W	10	28.8	F125W	12	28.6
F814W	42	29.1	F140W	10	28.6
			F160W	24	28.7

A370: first gravitational arc ever discovered in a cluster (Soucail et al. 1987; Lynds & Petrosian, 1986)

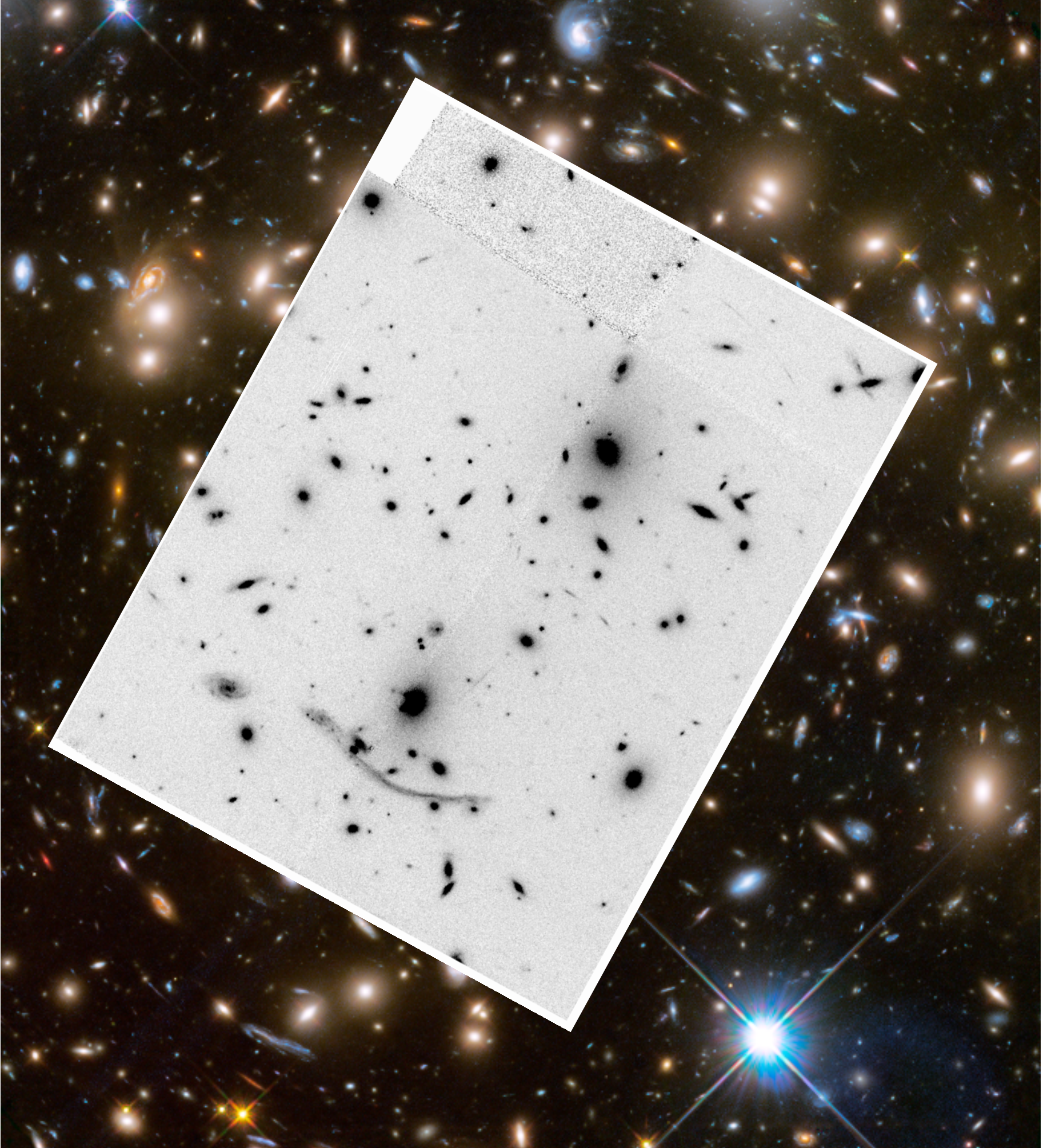


CFHT (R-band, 1985)

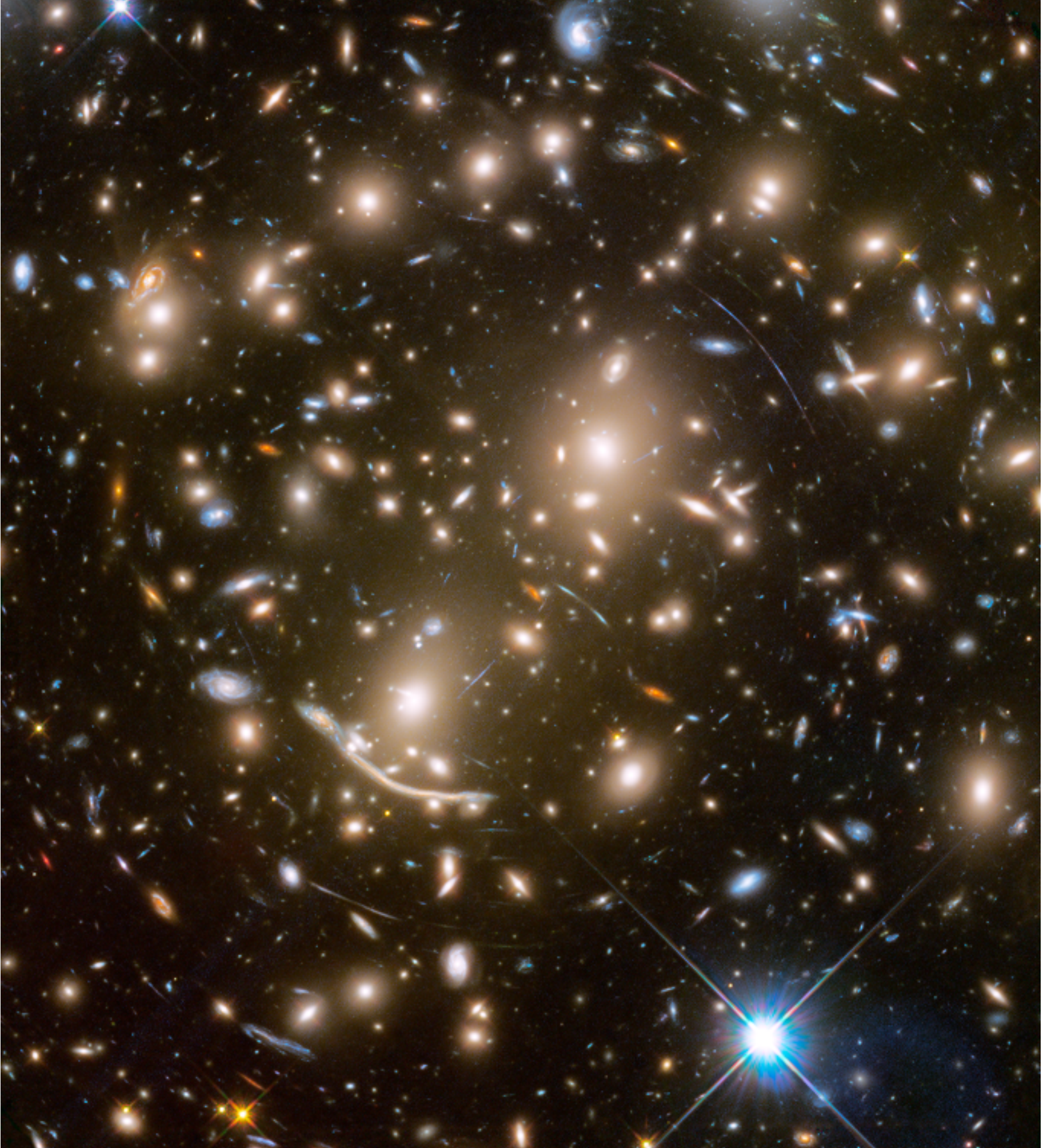


HST WFPC2 (F675W, 1995)

*A370 after the
FF program*



*A370 after the
FF program*



1. Before HFF ...

Previous GL Analysis :
Zitrin et al. 2013, *ApJ*, 762, 30

- 34 SL multiple images
- no WL data

PreHFF GL analysis :
Johnson et al. 2014, *arXiv 1405.0222*
Coe et al. 2014, *arXiv 1405.0011*
Richard, Jauzac et al. 2014, *MNRAS*, 444, 268

- 47 SL multiple images
- ~ 50 WL gal.arcmin $^{-2}$

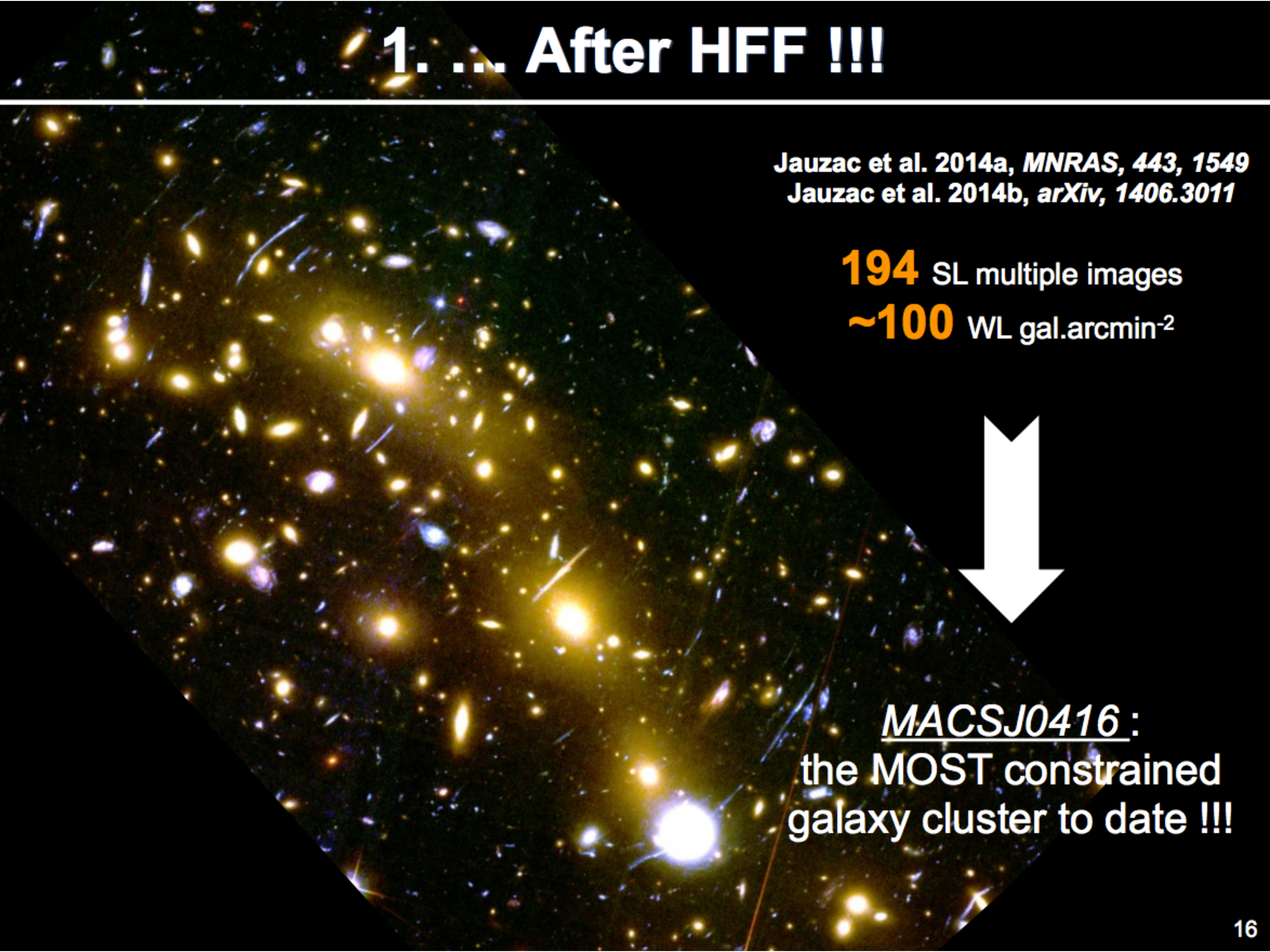
1. After HFF !!!

Jauzac et al. 2014a, *MNRAS*, 443, 1549
Jauzac et al. 2014b, *arXiv*, 1406.3011

194 SL multiple images
~100 WL gal.arcmin⁻²

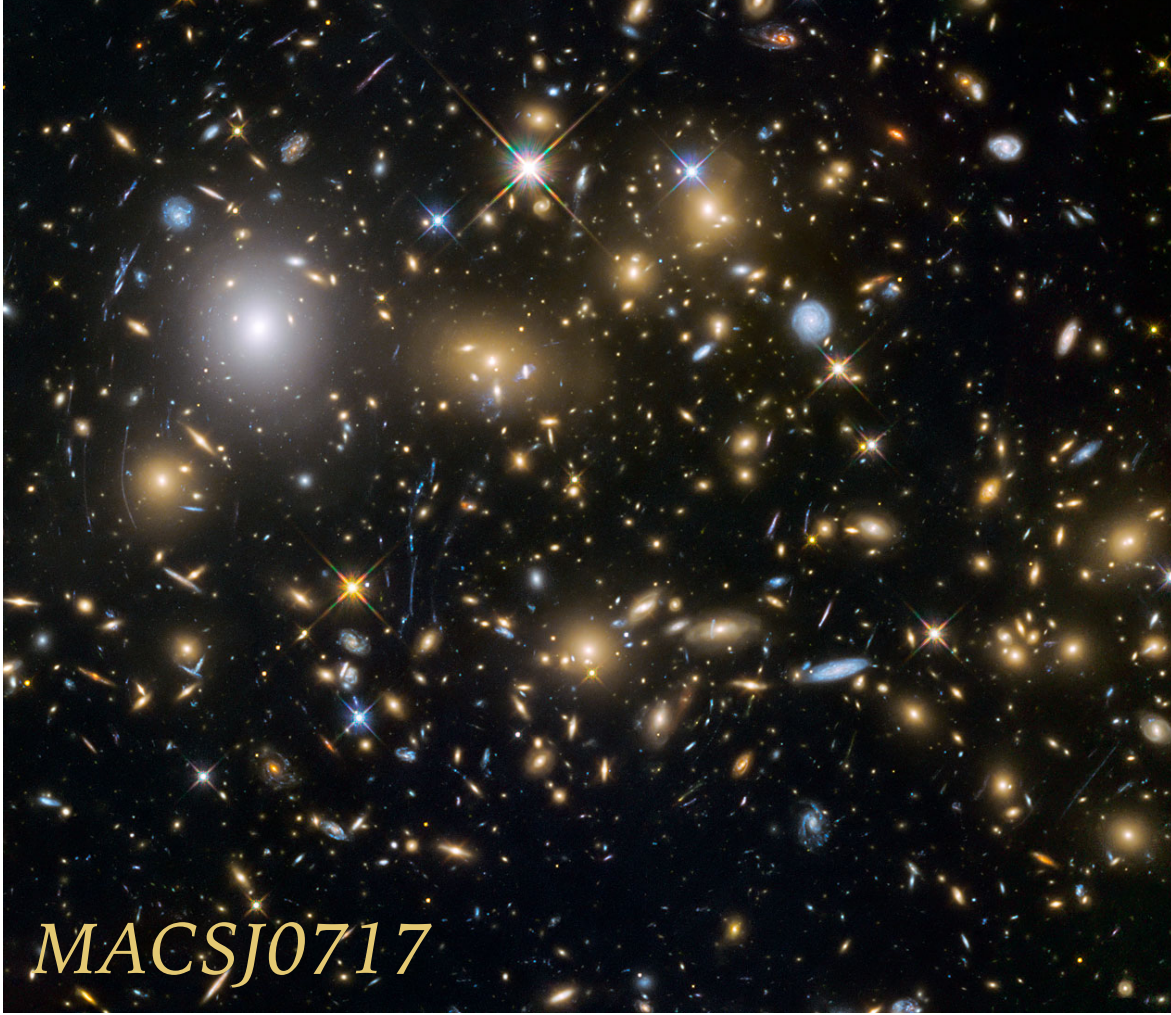


MACSJ0416:
the MOST constrained
galaxy cluster to date !!!

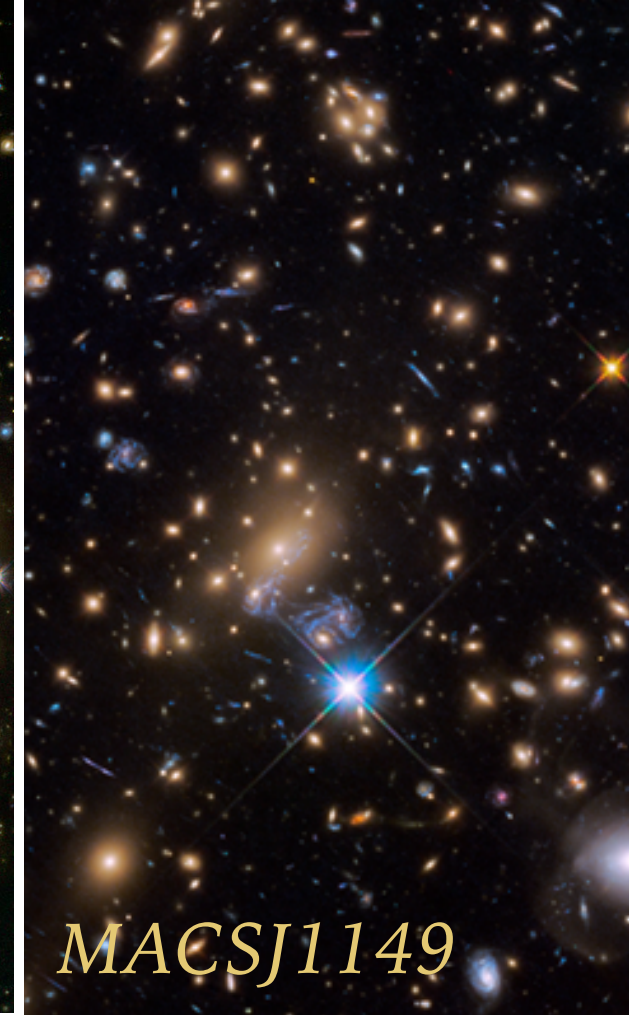




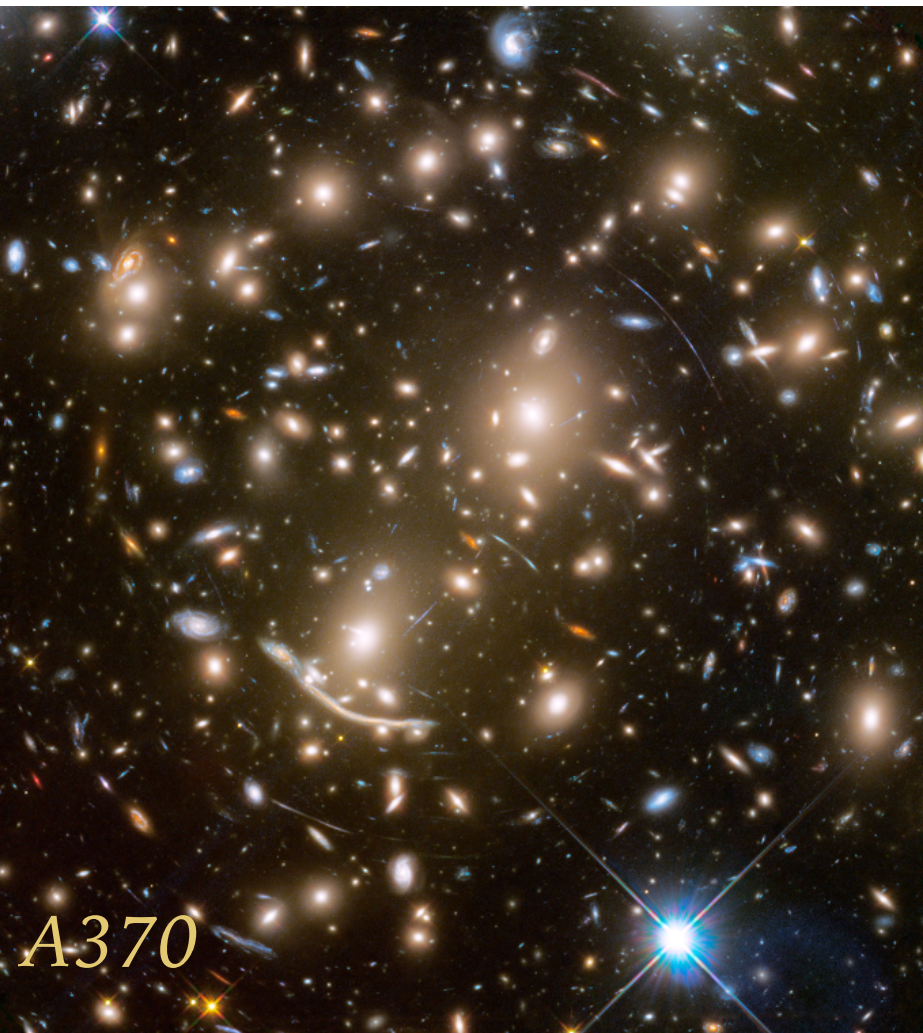
MACSJ0416



MACSJ0717



MACSJ1149



A370



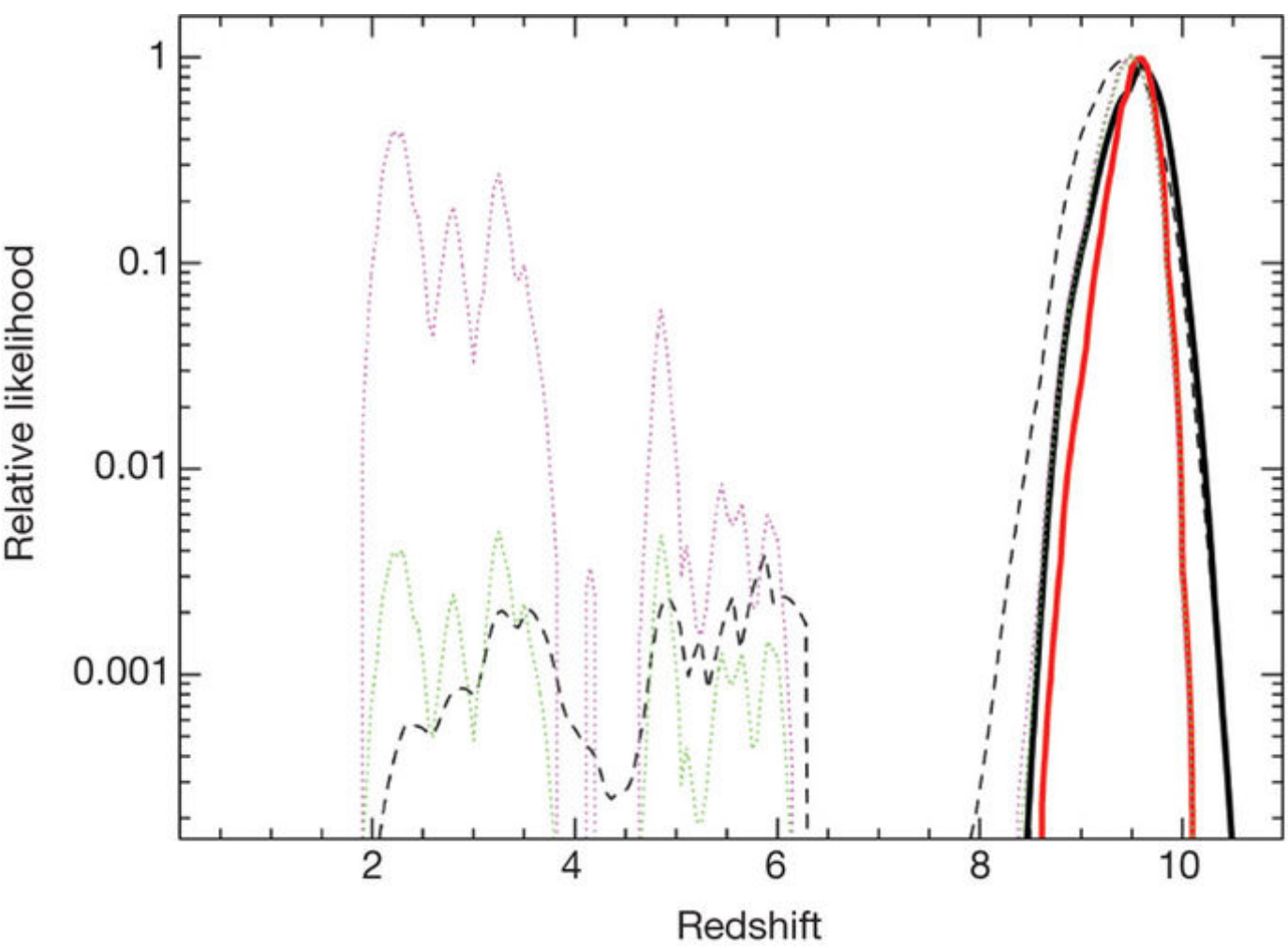
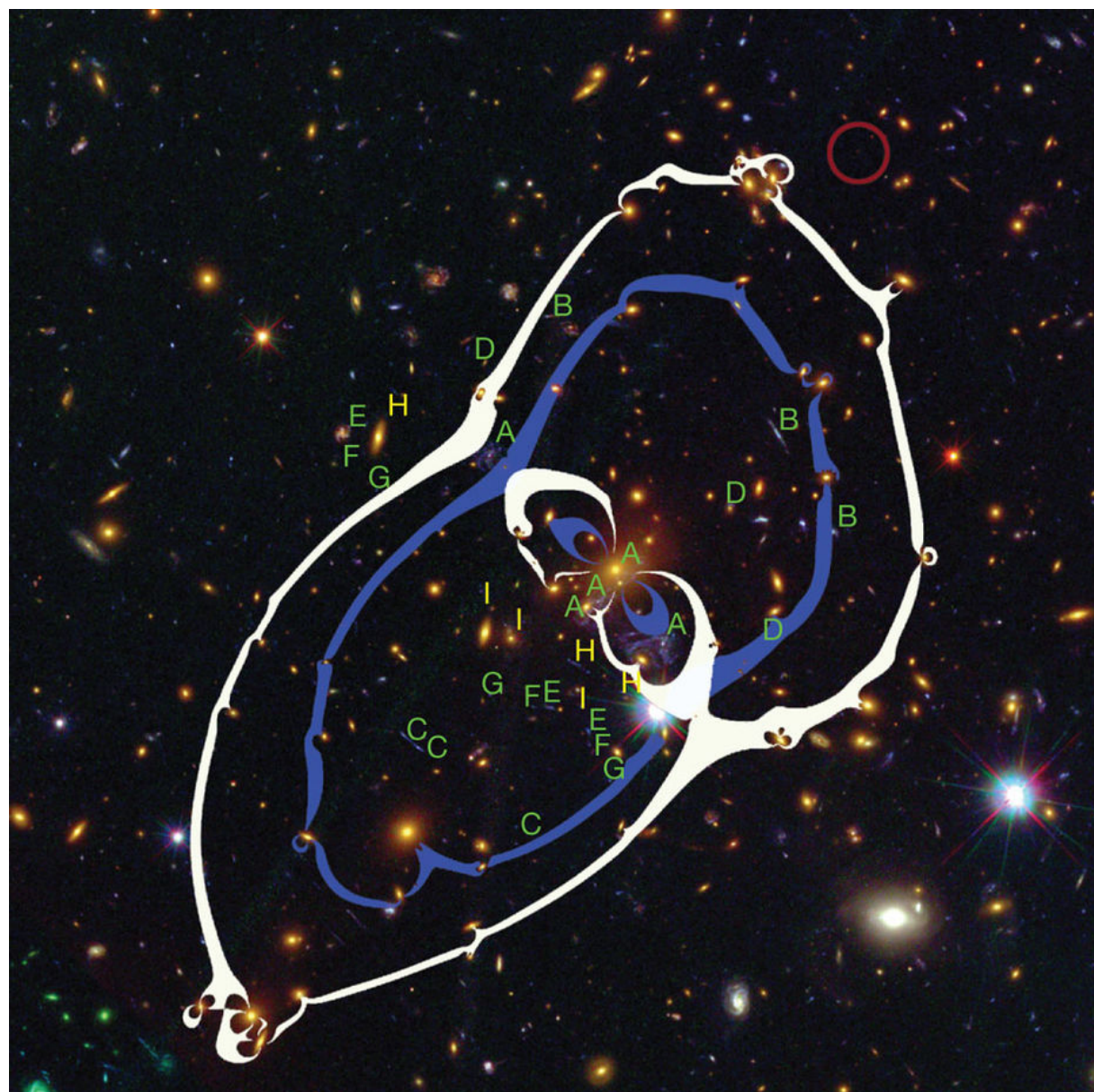
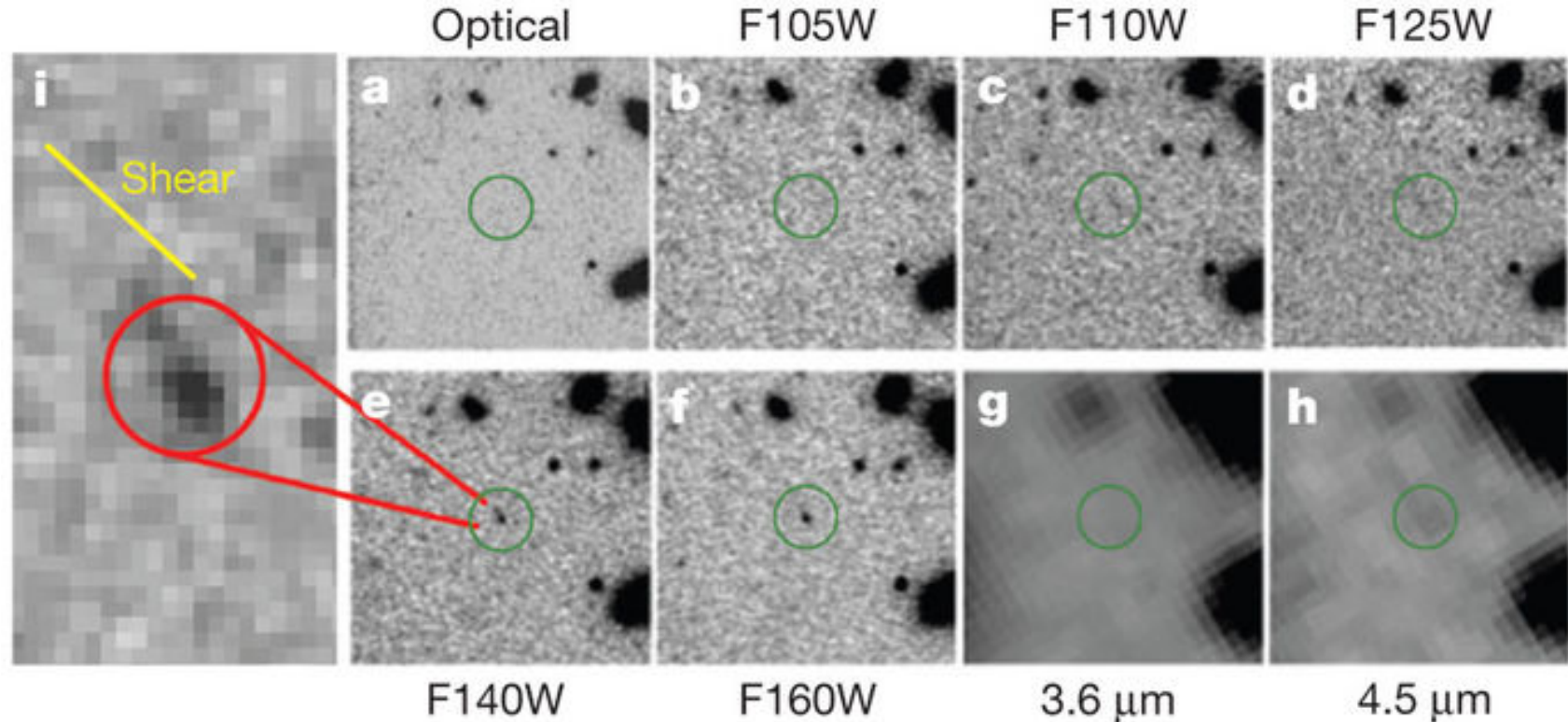
A2744



AS1063

COSMIC TELESCOPES

Some of the most distant sources where discovered using cosmic telescopes
(Zheng et al., 2012, $z \sim 9.6$;
Coe et al. 2013, $z \sim 10.8$)



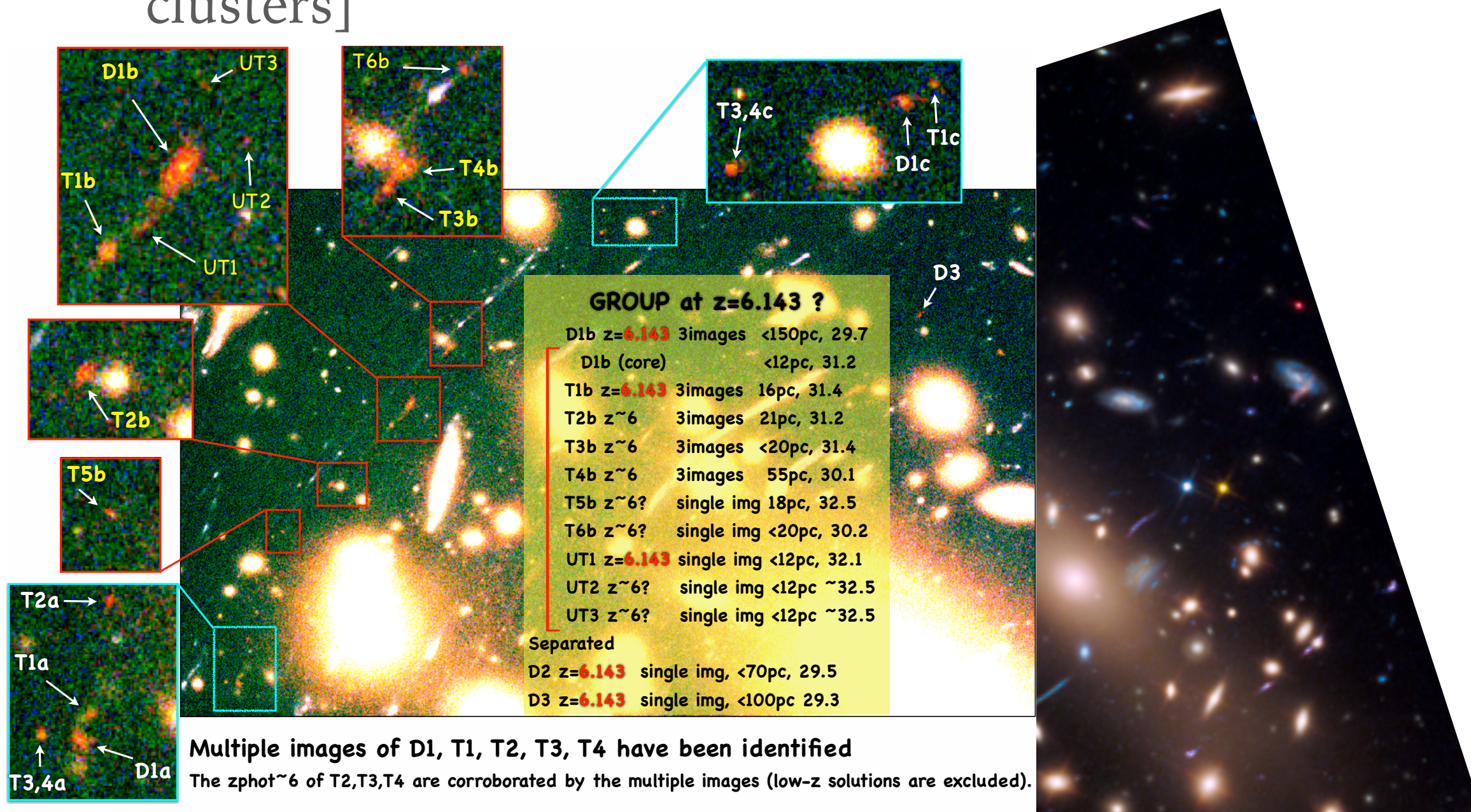
COSMIC TELESCOPES

- use the enormous magnification power of galaxy clusters to detect and characterize distant, intrinsically small and/or faint sources [re-ionization, build-up of galaxies, proto-globular clusters]



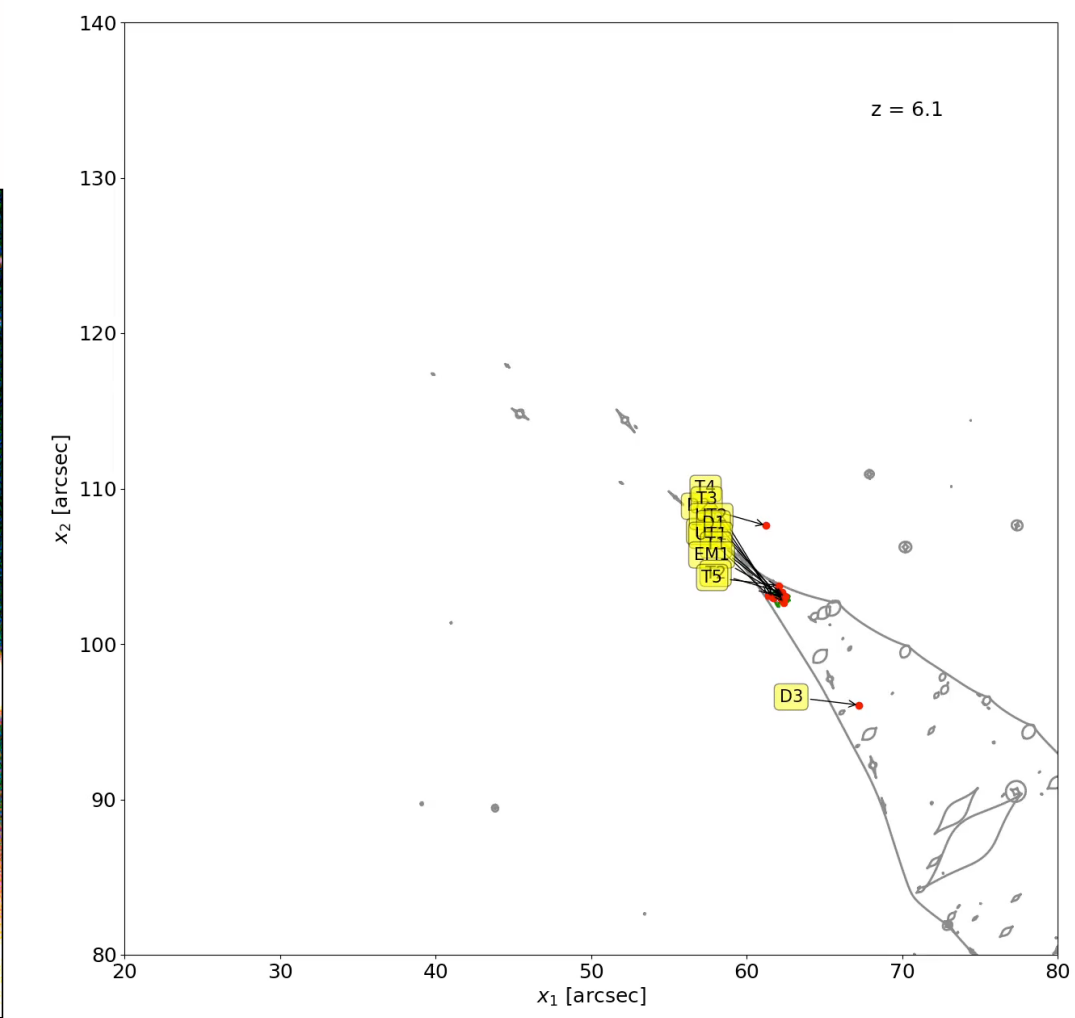
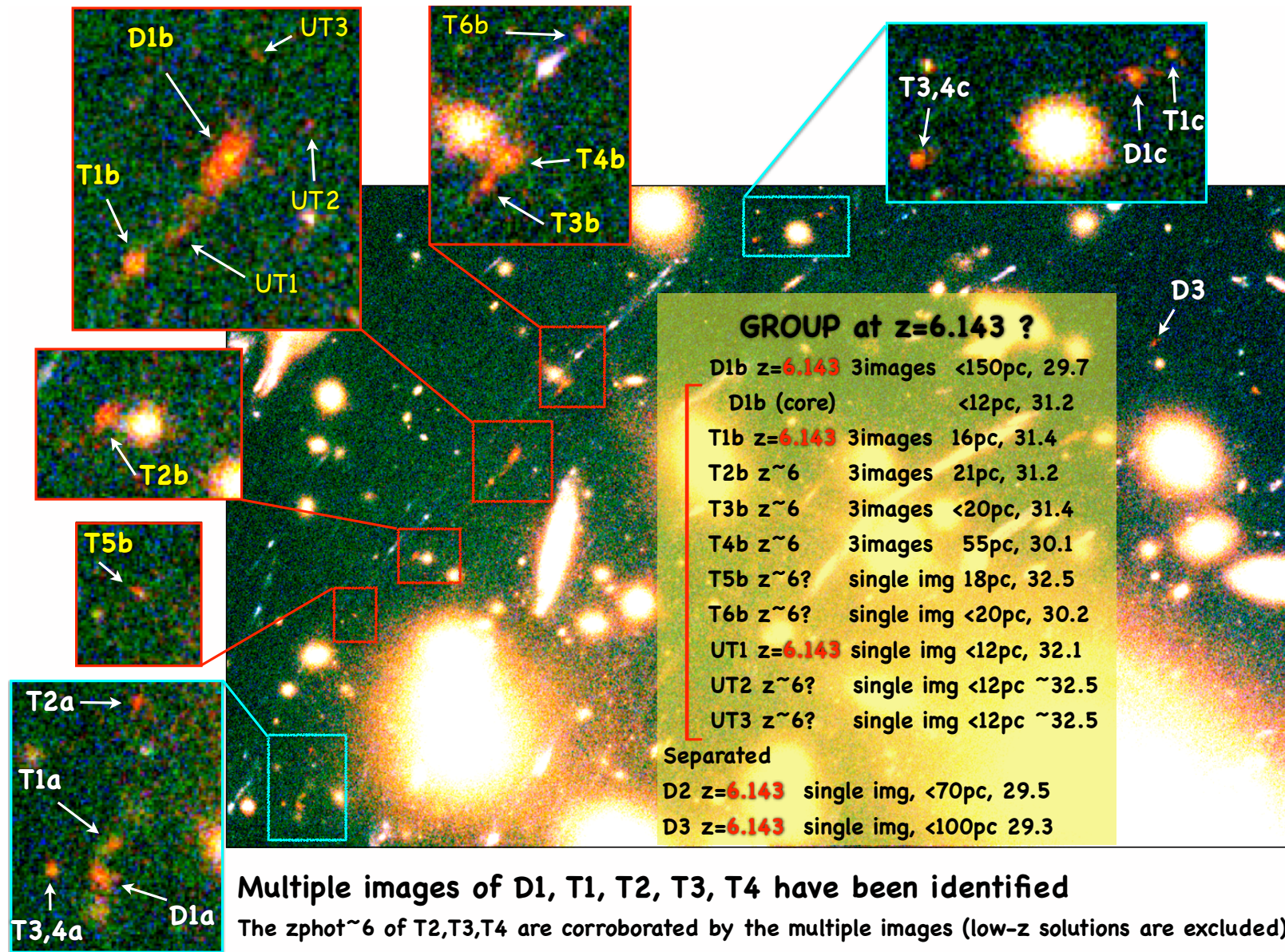
COSMIC TELESCOPES

- use the enormous magnification power of galaxy clusters to detect and characterize distant, intrinsically small and/or faint sources [re-ionization, build-up of galaxies, proto-globular clusters]



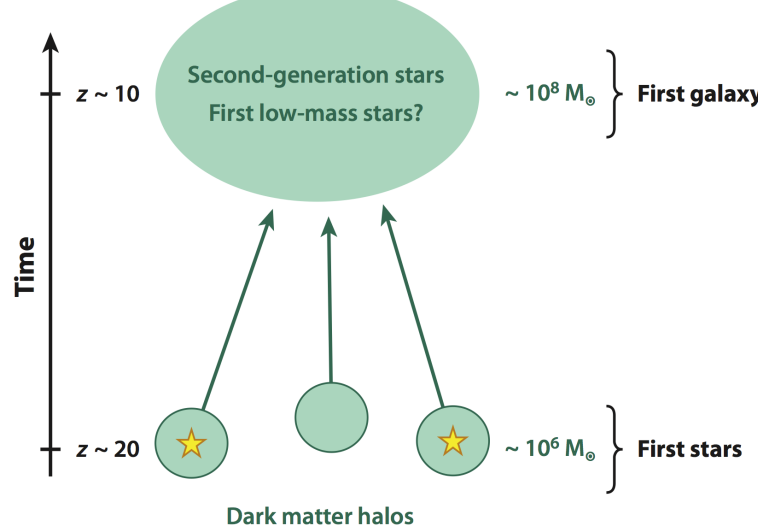
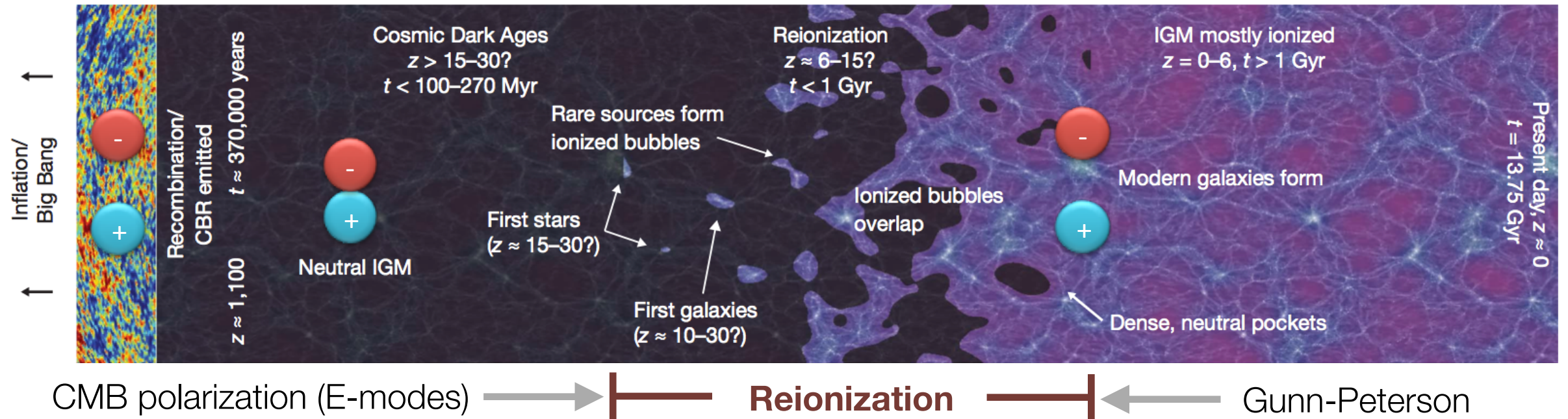
COSMIC TELESCOPES

- use the enormous magnification power of galaxy clusters to detect and characterize distant, intrinsically small and/or faint sources [re-ionization, build-up of galaxies, proto-globular clusters]



COSMIC REIONIZATION

Robertson et al. 2010

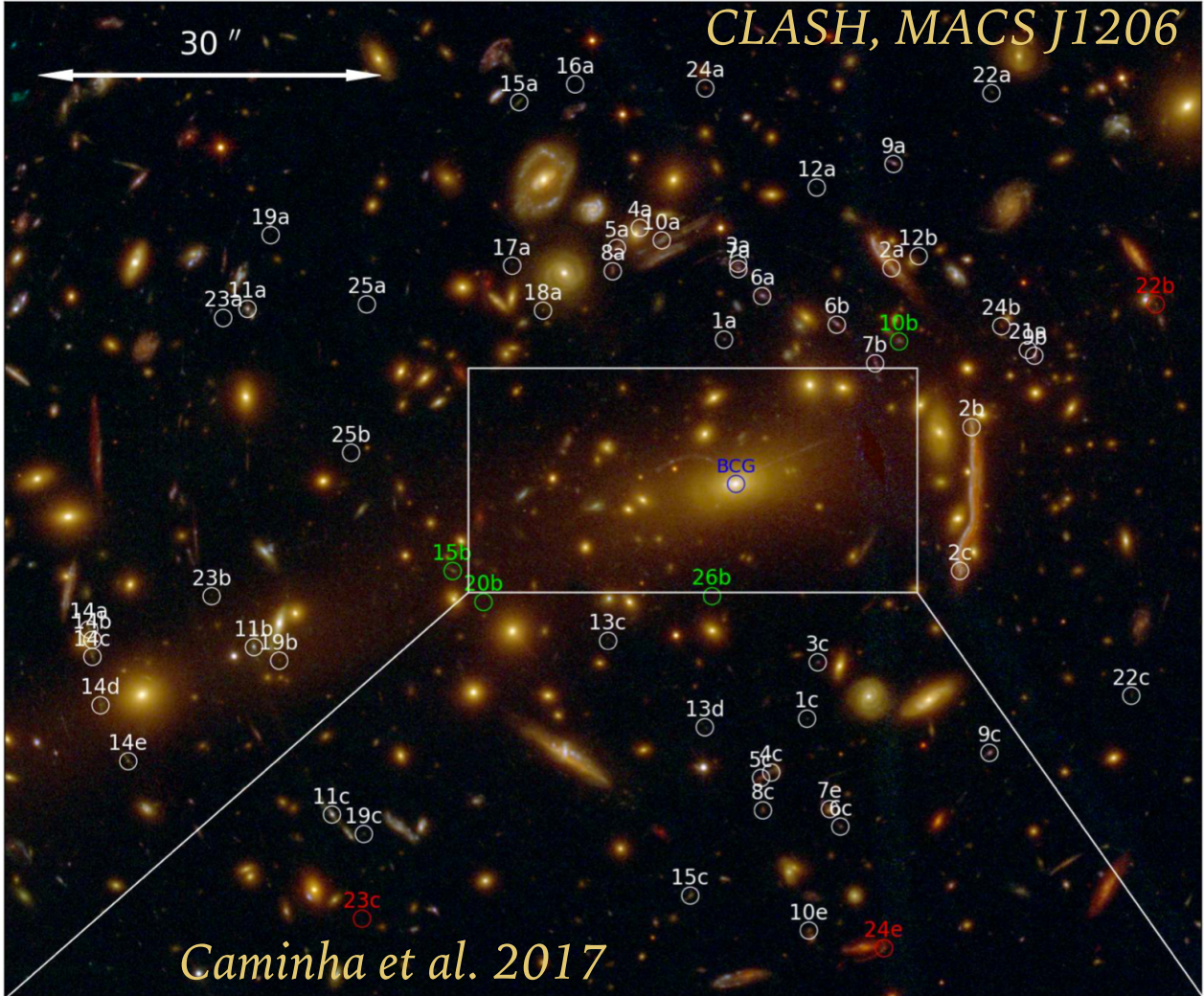


Universe has been re-ionized between $z \sim 15$ and $z \sim 8$

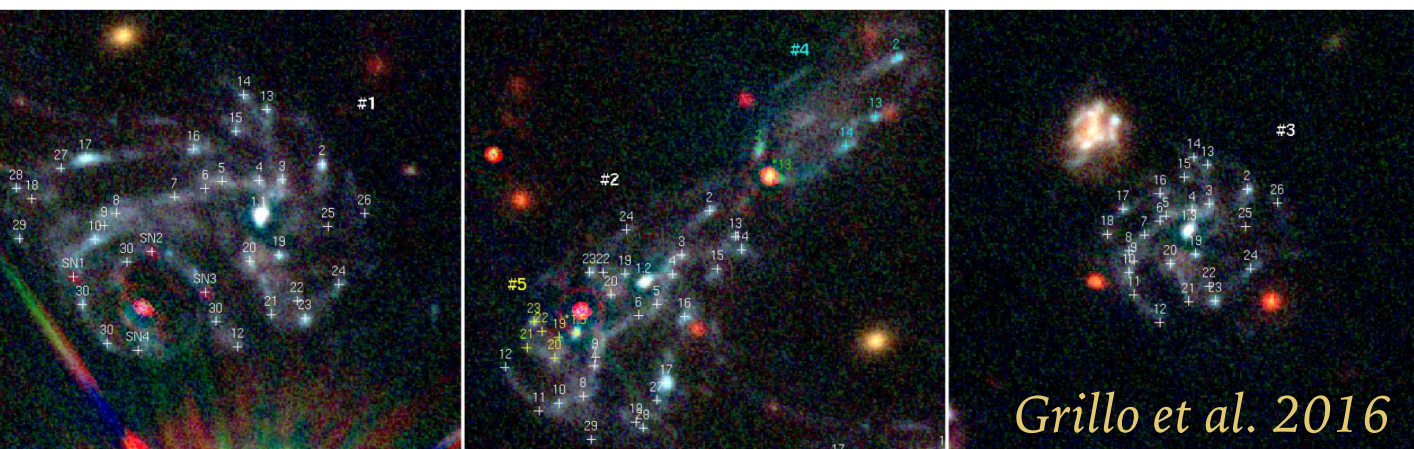
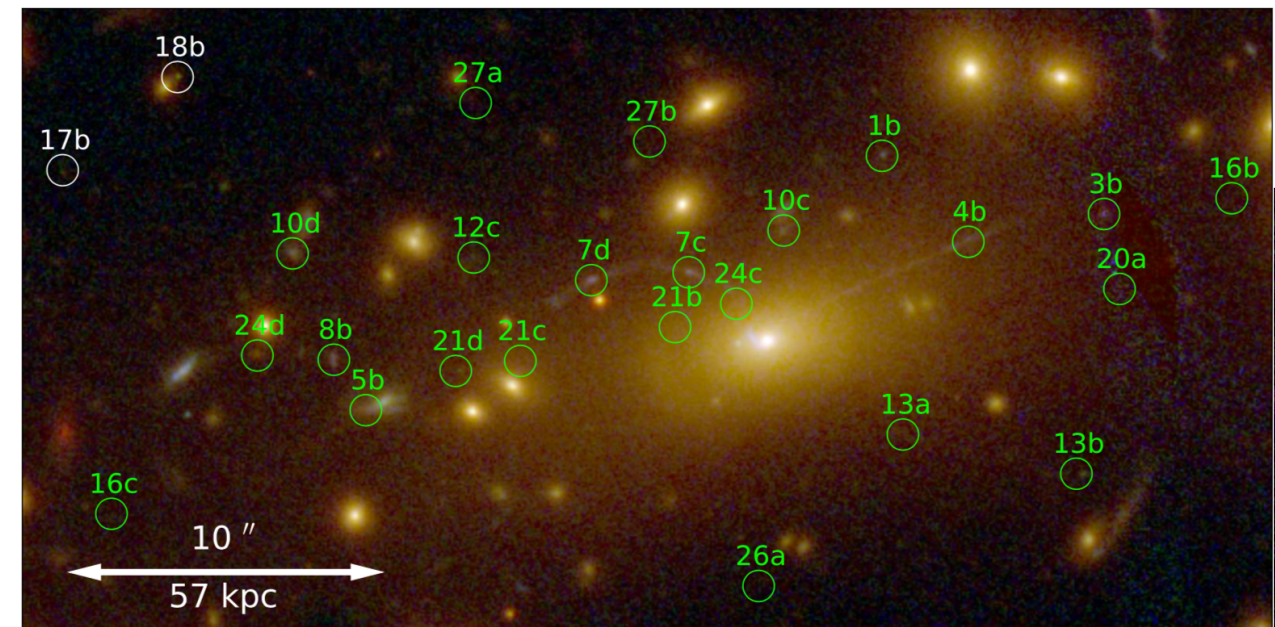
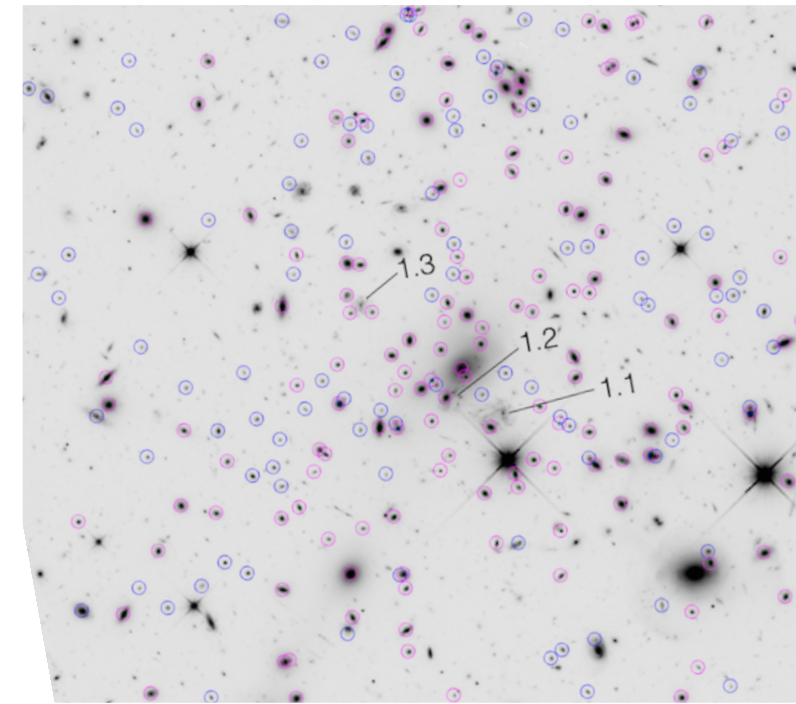
How and when did the first galaxies form?

Where they responsible for the re-ionization of the universe?

CLUSTER PARAMETRIC MODELS



- mostly positional constraints: several families of multiple images from sources covering a range of redshifts
- image deformation is sometimes usable



SUBSTRUCTURES

- The complexity of cluster lenses is way larger than galaxy lenses.
- For example: asymmetric mass distributions, multiple halos, substructures. The number of free parameters can be very large.
- Some tricks can be used to reduce them. For example: cluster substructures, traced by galaxies, can be modeled with scaling relations linking their lensing properties to some observable (e.g. the luminosity)

$$\sigma = \sigma_\star \left(\frac{L}{L_\star} \right)^{1/4}$$

$$r_t = r_{t,\star} \left(\frac{L}{L_\star} \right)^\eta$$

SUBSTRUCTURES

- The complexity of cluster lenses is way larger than galaxy lenses.
- For example: asymmetric mass distributions, multiple halos, substructures. The number of free parameters can be very large.
- Some tricks can be used to reduce them. For example: cluster substructures, traced by galaxies, can be modeled with scaling relations linking their lensing properties to some observable (e.g. the luminosity)

$$\sigma = \sigma_* \left(\frac{L}{L_*} \right)^{1/4}$$
$$r_t = r_{t,*} \left(\frac{L}{L_*} \right)^\eta$$

LENS OPTIMIZATION

- lensing likelihood:
- minimization of χ^2
to find the best \mathbf{p} fitting the data
- iterate between image and source plane
- or optimization in the source plane
- Lenstool (Kneib et al. 1998; Jullo et al. 2010); GLAFIC (Kawamata et al. 2016)

$$\mathcal{L} = \Pr(D|\mathbf{p}) = \prod_{i=1}^N \frac{1}{\prod_{j=1}^{n_i} \sigma_{ij} \sqrt{2\pi}} \exp -\frac{\chi_i^2}{2}$$

Number of systems

Number of images

Contribution from single system

$$\chi_i^2 = \sum_{j=1}^{n_i} \frac{[\vec{\theta}_{obs}^j - \vec{\theta}_{\mathbf{p}}^j]^2}{\sigma_{ij}^2}$$

$$\vec{\beta}_{\mathbf{p}}^j = \vec{\theta}_{obs}^j - \vec{\alpha}(\vec{\theta}_{obs}^j, \mathbf{p})$$

$$\vec{\beta}_{\mathbf{p}}^j = \vec{\theta}_{\mathbf{p}}^j - \vec{\alpha}(\vec{\theta}_{\mathbf{p}}^j, \mathbf{p})$$

$$\chi_{S,i}^2 = \sum_{j=1}^{n_i} \frac{[\beta_{\mathbf{p}}^j - \langle \beta_{\mathbf{p}}^j \rangle]}{\mu_j^{-2} \sigma_{ij}^2}$$

MODEL OF MACSJ1206 (CAMINHA ET AL. 2017)

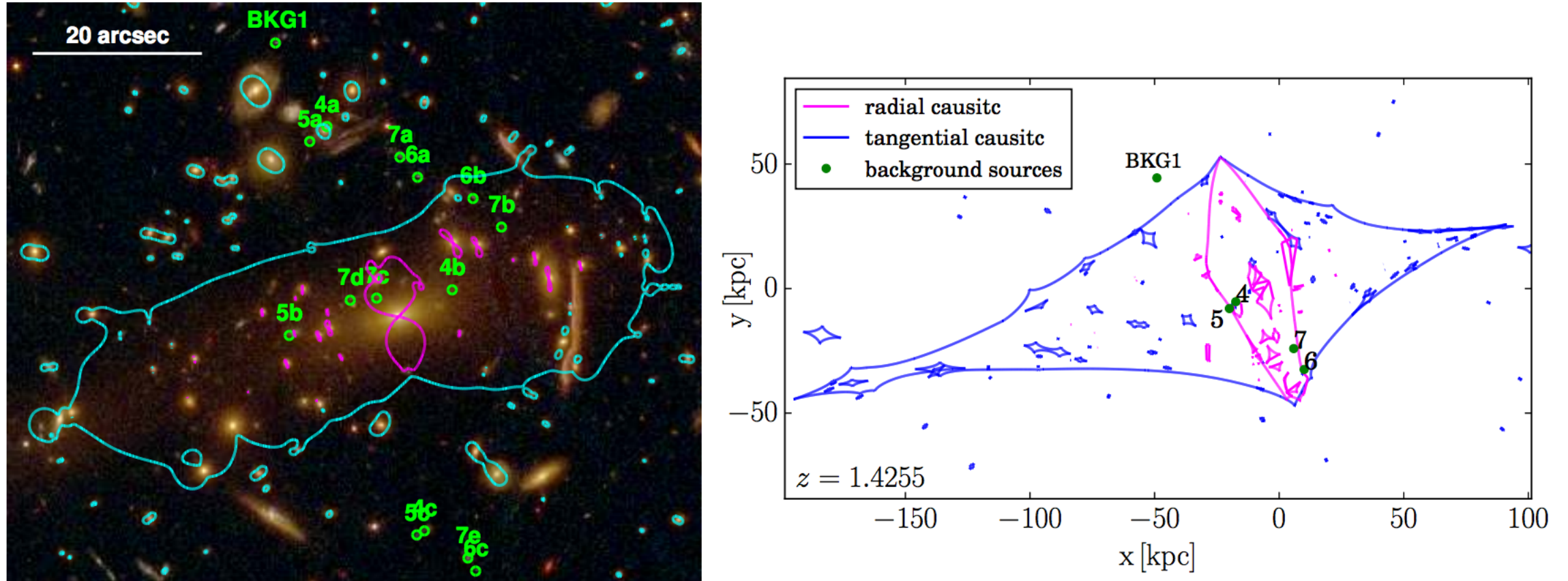


Fig. 6: Critical curves and caustics of the reference model P3 ε for a source at $z_{src} = 1.4255$ (the mean redshift values of the sources). Left panel: Tangential (cyan) and radial (magenta) critical lines on the image plane. The green circles show the observed positions of the multiple images belonging to the four families within $\Delta z \leq 0.0011$. BKG1 is a background galaxy not multiply lensed by MACS 1206. Right panel: Tangential (cyan) and radial (magenta) caustics on the source plane, and the reconstructed positions of the background sources.

OUTCOME

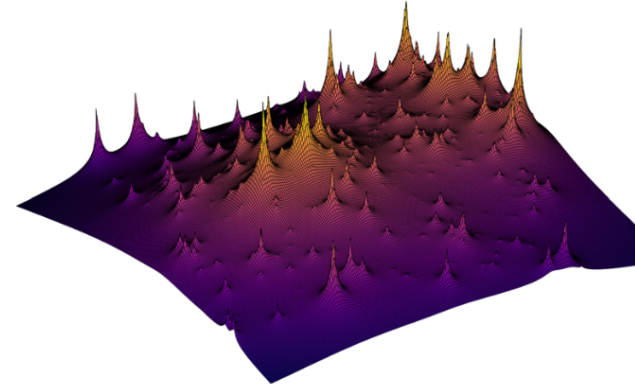


Figure 27. 3D visualization of the lensing-derived substructure distribution for Abell 2744.

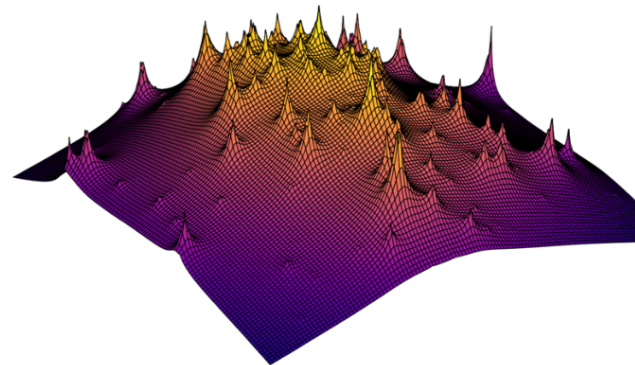


Figure 28. 3D visualization of the lensing-derived substructure distribution for MACSJ 0416.

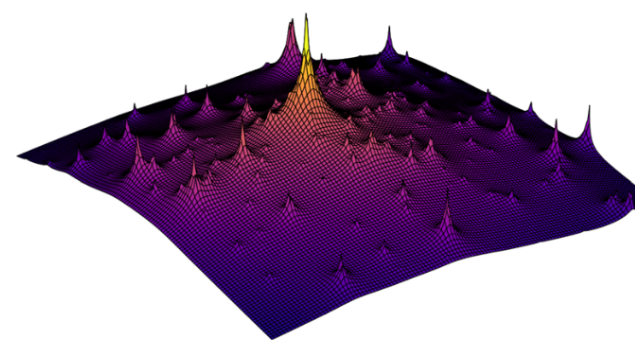


Figure 29. 3D visualization of the lensing-derived substructure distribution for MACSJ 1149.

